Meccanica **31:** 235–271, 1996.

Three-dimensional Shapes of Looped DNA

EUGENE L. STAROSTIN
Russian Academy of Sciences, Keldysh Institute of Applied Mathematics, 4 Miusskaya Sq.; 125047, Moscow, Russia

(Received: 21 February 1995; accepted in revised form: 5 October 1995)

Abstract. The equilibrium shapes of a closed DNA are investigated by employing a model of a thin, homogeneous, isotropic, linearly elastic rod of circular cross section. An equilibrium configuration of such an initially straight and twisted rod, submitted to external forces and moments at its ends only, obeys equations identical to those governing the rotation of a symmetric gyrostat spinning about a fixed point in a gravitational field (the Kirchhoff analogy). To represent the equilibrium of the looped DNA, the model rod must be smoothly closed into a ring. The corresponding BVP results in a system of four nonlinear equations with respect to four parameters. The perturbation analysis and the parameter continuation approach are used to find nonplanar solutions. The conformation change is discussed for various values of parameters.

Sommario. Si analizzano le configurazioni di equilibrio di una molecola chiusa di DNA per mezzo di un modello di trave sottile, omogenea, isotropa e linearmente elastica, con sezione circolare. La configurazione di equilibrio di una tale trave, inizialmente rettilinea e poi ritorta, soggetta a forze esterne e momenti solo alle sue estremità, è descritta dalla soluzione di equazioni identiche a quelle che governano il moto di un girostato simmetrico in rotazione intorno ad un punto fisso in un campo gravitazionale (l'analogia di Kirchhoff). Per poter rappresentare l'equilibrio del cappio di DNA, il modello di trave deve essere racchiuso in un anello, Il corrispondente problema al contorno consiste in un sistema di quattro equazioni nonlineari rispetto a quattro parametri. Le soluzioni del problema fuori del piano vengono ottenute tramite l'analisi perturbativa ed una procedura di continuazione al variare di un parametro. Si discutono le modifiche di configurazione del sistema per diversi valori dei parametri.

Key words: DNA double helix, Thin rod, Equilibrium, Kirchhoff's analogy, Elasticity, Bifurcation

> 'It is not easy to think clearly about the way in which double-stranded DNA twists into various coils and supercoils'.
>
> F.H.C. Crick [1].

1. Introduction

A molecule of deoxyribonucleic acid, DNA, is usually represented by two chains of complementary nucleotides which wind around a common axis and form a right-handed double helix. The double helix of DNA was discovered by James D. Watson and Francis H.C. Crick in 1953. The radius of the helix is about 10 Å and the length of the DNA may achieve 10^4 Å or even more. Approximately 10 base pairs correspond to one turn of the helix in the relaxed state [2].

Over more than two decades, a number of papers have appeared, which deal with the subject of the global structure of DNA (e.g. [1]–[10]).

Two models are used when studying properties of a DNA as a whole.

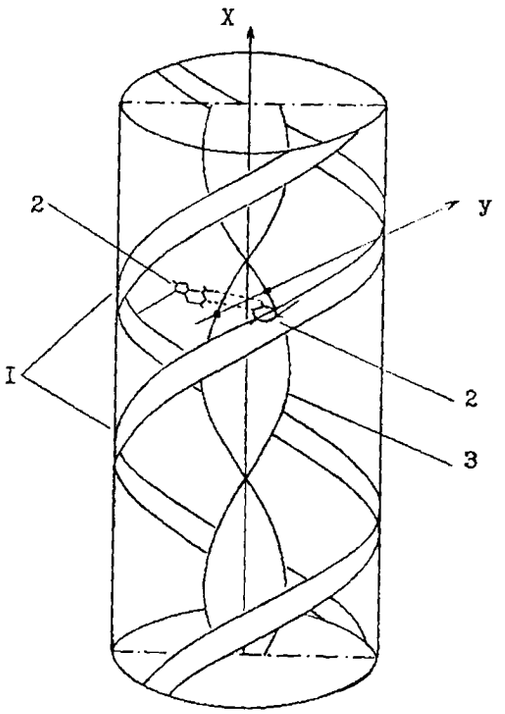

Figure 1. The model of DNA. 1, two sugar-phosphate backbones; 2, paired nucleotide bases; 3, a twisted ribbon; x, the helical axis; y, the dyad axis.

From the mathematical point of view, the molecule is a narrow, infinitesimally thin ribbon with axis following the axis of the helix and its surface lies perpendicular to the dyad axes defined by the base pairs (Figure 1) [1], [3].

Mechanical properties of DNA are usually studied by modelling it as a thin elastic rod. The intersection of a ribbon surface with the rod gives two winding antipodal lines. They may be assigned opposite directions. This reflects opposite spatial orientations of bases in the two polynucleotide chains. The ribbon and the rod may bend and twist (Figure 2).

The DNA molecules are known to exist in either linear or circular form. Each of two polynucleotide chains that constitute the double helix is looped in the closed DNA molecule. In 1965 J.Vinograd introduced the concept of a superhelicity or supercoiling of DNA. The superhelicity may be observed in experiments. It arises from the fact that the winding rate of the helix about its central axis is usually less in the circular molecule than in the same molecule when it is in the linear relaxed form. Therefore, in this case, the looped DNA can wind in space to form a superhelix of a higher order. Then it is said to be supercoiled or superhelical. A large proportion of DNAs take a supercoiling form at least once in their life cycles.

Specialized enzymes were discovered that control superhelicity of DNA. They are called topoisomerases. Supercoiling is a biologically important form of DNA. One example shows that it is true: if the gyrase, the enzyme that causes negative supercoiling, is destroyed then replication of the DNA cannot proceed. Superhelicity was observed in molecules containing various number of base pairs – from 350 to 1 750 000.

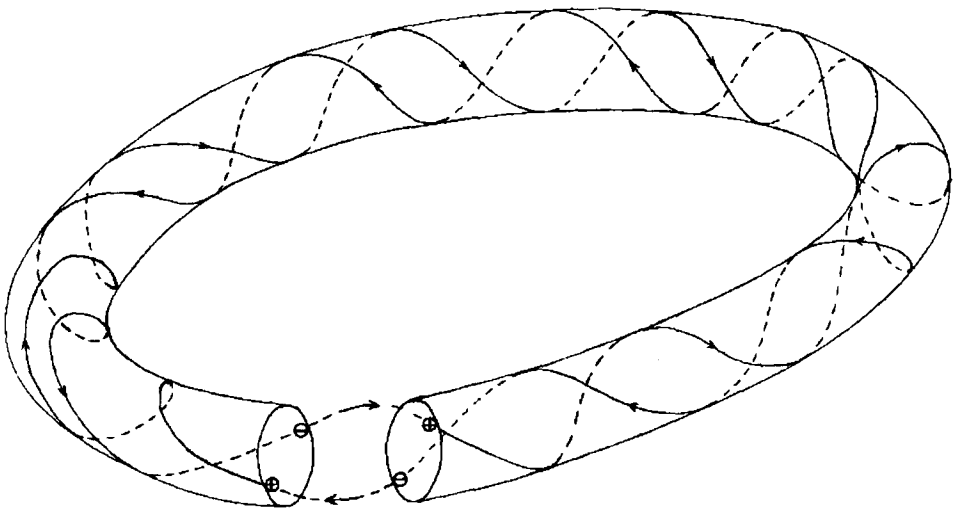

Figure 2. A closed DNA. The two winding lines of opposite direction are the edges of the model ribbon and they must join themselves.

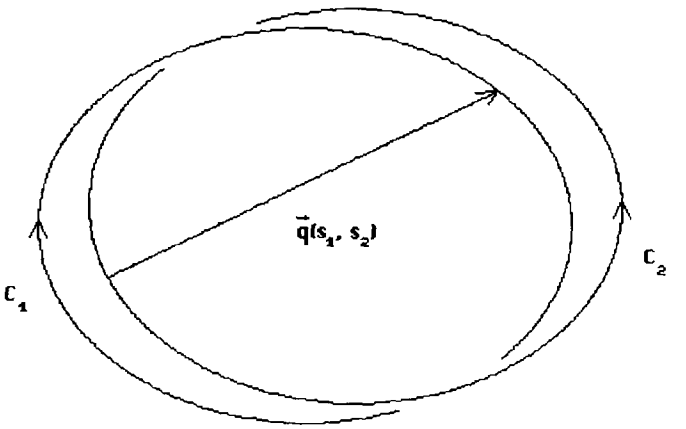

Figure 3. To the integral formula for the linking number of two loops; $\mathbf{q}(s_1, s_2)$ is a continuous vector function defined for loops C_1 and C_2.

A number of works were devoted to investigations of spatial conformations of the DNA molecule by employing the thin elastic rod model. The rod model is the *elastica* and its equilibrium equations were given by Euler, Kirchhoff and Clebsch. It is extensively described in [11], where planar non-closed equilibrium shapes are presented.

Benham [4] treated a homogeneous isotropic rod of circular cross section by applying the Kirchhoff analogy. He gave some considerations for possible shapes of an elastic molecule. The elastic model was also studied in [5]. A more detailed analysis can be found in [6]; it contains the ring closure conditions. The closed conformations were studied in [2], [8]. The variational approach was applied to obtain the equilibrium equations of the model rod. An elastic energy extremum was searched subject to the smooth closure constraint with a fixed linking number. The simple plane circular and 8-shaped forms were found. An approach based

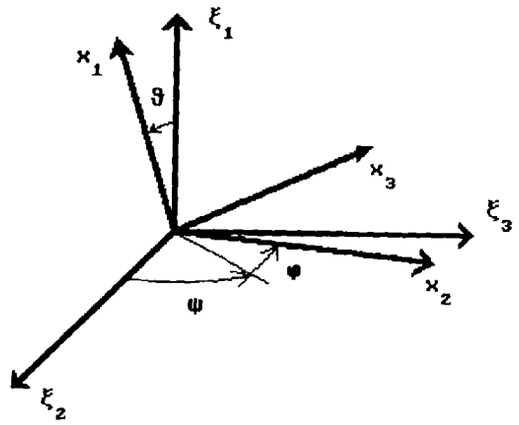

Figure 4. The Euler angles ψ, φ, and ϑ specify the attitude of the principal axes of bending and twisting $x_1x_2x_3$ with respect to the coordinate system $\xi_1\xi_2\xi_3$ fixed in space. The axis x_1 is along the central axis of DNA. The direction of the axis ξ_1 is coincident with the direction of the end force $P\gamma$.

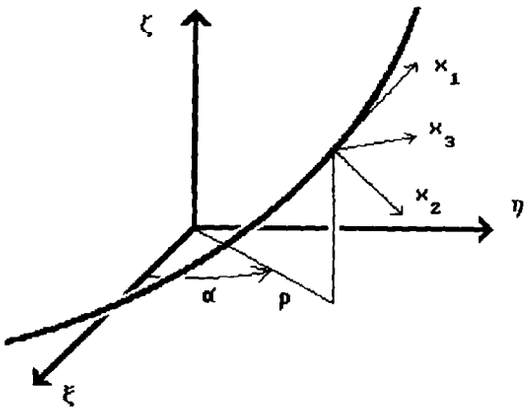

Figure 5. The cylindrical coordinates ρ, α, and ζ of the central axis of DNA.

on the ideas of Fuller and Benham was developed in [7] where considerable numerical results were presented for spatial conformations of DNA. However, closed molecules were not dealt with.

Mention should be made of recent works devoted to shapes of the thin elastic rod as well as to its dynamics [12], [13]. The variational technique is applied.

Possible shapes of a closed elastic rod were classified in [14] by using the group theory.

2. Some Related Mathematical Concepts

The polynucleotide chains are closed in a looped DNA [15]. Each of the two chains may join only with itself – and not with the other (an analog of the Möbius strip is impossible for DNA).

The linking number Lk indicates how many times one closed loop encircles the other and it is given by the Gauss integral [2]:

$$Lk = \frac{1}{4\pi} \int_{C_1} \mathrm{d}s_1 \int_{C_2} \mathrm{d}s_2 \, \frac{1}{|\,\mathbf{q}\,|^3} \det\left(\frac{\partial \mathbf{q}}{\partial s_1}, \frac{\partial \mathbf{q}}{\partial s_2}, \mathbf{q}\right),$$

where $\mathbf{q}(s_1, s_2)$ is a vector function defined for two loops C_1 and C_2 (Figure 3).

The linking number value cannot change unless at least one loop is broken (nicked). From a practical point of view the problem can be solved effectively by using algorithms of the computational geometry. The algorithms of searching for projection points of spatial curves are widely used in the computer graphics. They can be applied for computation of linking numbers.

Two more numbers that describe the spatial configuration of the molecule may be introduced [2], [8].

The twisting number Tw counts how many times either loop twists around the central axis of the DNA.

$$Tw = \frac{1}{2\pi} \int_0^S \omega_1(s)\, \mathrm{d}s,$$

where ω_1 is a twisting rate of the polynucleotide chain, s is the arclength of the central axis, $0 \leq s \leq S$, S is the total length of the central axis.

Note that the twisting number may be defined for an arbitrary molecule (not necessary for a closed one).

For a closed ribbon, the difference between the linking of its edges and its twisting depends only on the shape of the central axis. Fuller [16] gave this quantity the name of writhing (Wr)

$$Wr = Lk - Tw. \tag{1}$$

The writhing is equal to zero for a planar closed curve or for a closed curve lying on a sphere.

In contrast to linking, neither twisting nor writhing are topological invariants and their values may vary continuously as the molecule changes its shape in space.

The basic relationship implies that by continuous deformation of a molecule when its writhing number changes, the twisting number must change correspondingly because the linking remains constant.

3. Mechanical Model of DNA Molecule

Adequate understanding of how DNA works is impossible without complete investigation of its large-scale, tertiary structure, of which the mechanical properties of the molecule are known to be important determinants.

Results of many experiments show that, in solution, the DNA molecule possesses properties of a linearly elastic rod. Therefore, it appears reasonable to treat DNA as a long thin homogeneous rod of circular cross section governed by the linear elasticity law [6], [7]. Such a rod is characterized by two parameters – torsional and bending stiffnesses, which will be denoted by B_{11} and B_{22}, respectively, and assumed to be constant along the rod. The torsional and bending stiffness values have been found experimentally a number of times [17]. In

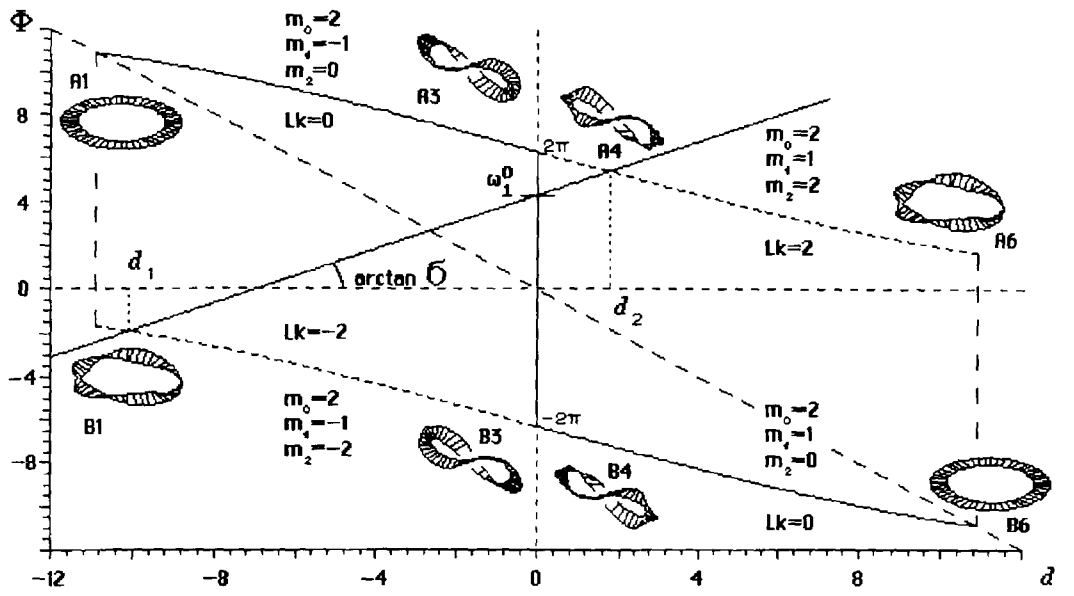

Figure 6. The function $\Phi(d)$ from (37) for $m_0 = 2$. Two branches are plotted. d_1 and d_2 are roots of Equation (36). ω_1^0 corresponds to the initial twisting. σ is the Poisson ratio.

particular, the bending stiffness dependence of the base pair composition has been studied in [18]. Below are presented the typical values [8] for the B-form of DNA

$$B_{11} = 2.2 \times 10^{-28}\text{Jm}, \qquad B_{22} = 2.7 \times 10^{-28}\text{Jm}.$$

For a cylindrical rod

$$B_{11} = \frac{\pi a^4 \mu}{2}, \qquad B_{22} = \frac{\pi a^4 E}{4},$$

where a is the cross section radius, E the Young modulus, μ the shear modulus (the Lamé coefficient) [19]. For $a = 10^{-9}m$, one can find

$$E = 3.5 \times 10^8 N\text{m}^{-2}, \qquad \mu = 1.4 \times 10^8 N\text{m}^{-2}.$$

This gives the Poisson ratio $\sigma = \frac{E}{2\mu} - 1 \approx 0.23$.

Notice that the values of E and μ may vary essentially with the chemical composition of the environment. For example, the Young modulus is halved as the concentration of NaCl reduces from 0.0005 M to 1 M [8].

3.1. The Elastic Rod Equilibrium Equations. The Kirchhoff Analogy

The equilibrium state of a curved and twisted rod is described by a system of differential equations [11], [20]

$$\frac{\mathrm{d}\mathbf{F}}{\mathrm{d}s} - \mathbf{f} = 0, \qquad \frac{\mathrm{d}\mathbf{M}}{\mathrm{d}s} + \mathbf{m} - \tau \times \mathbf{F} = 0. \tag{2}$$

Here, $\mathbf{F}$ is the resultant of all the forces acting in the cross section, $\mathbf{M}$ the moment of these forces, $\mathbf{f}, \mathbf{m}$ the densities of the distributed forces and moments, respectively, τ the unit vector

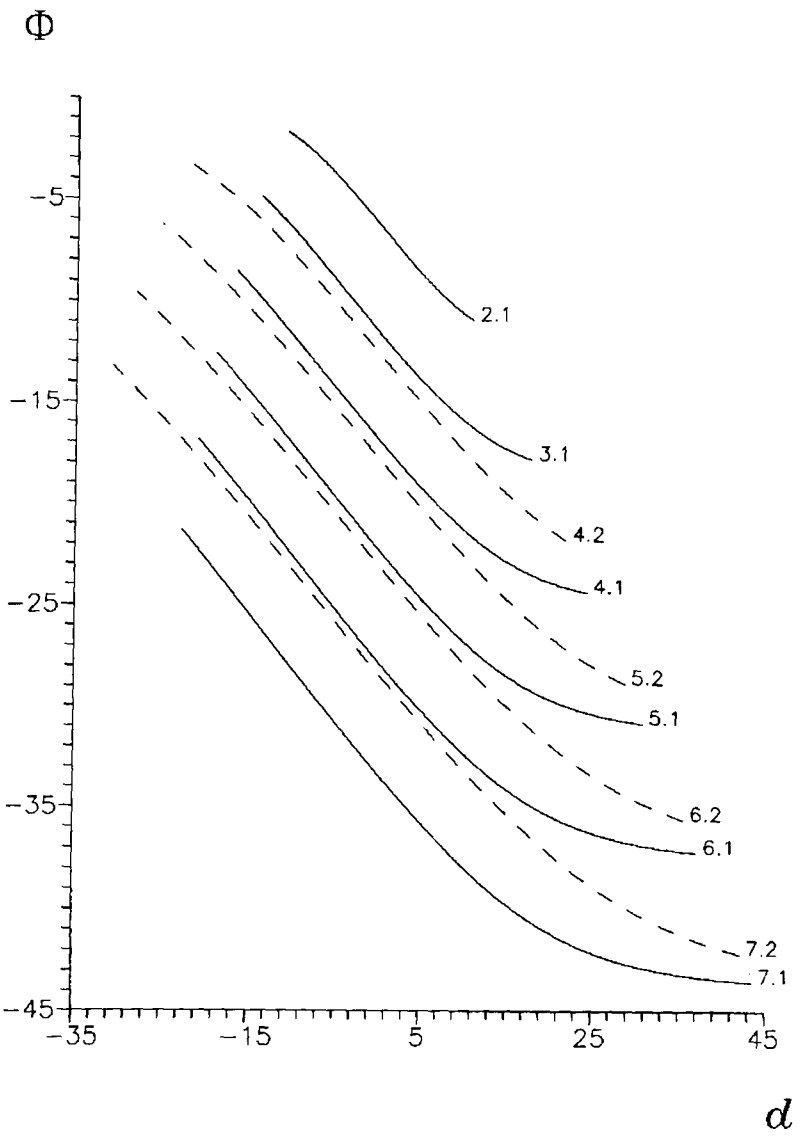

Figure 7. The functions $\Phi(d)$. The curves are marked with two numbers: the first indicates m_0, the second – m_1 (its value is given for starting non-perturbed solutions). Two series are presented for $m_1 = 1$ (solid lines) and $m_1 = 2$ (dashed lines). All the curves $\Phi(d)$ are shown continuous.

along the tangent to the central axis, s the arc coordinate along the central axis (its extension is neglected).

The cross section is assumed to remain plane and orthogonal to the central axis after deformation.

We introduce the principal axes of bending and twisting for a deformed state: direct axis x_1 along the tangent to the central axis (i.e., along τ) and axis x_2 along the tangent to the line, into which one of the principal central inertia axes of the cross section for the non-deformed state turns; x_3 supplements the system up to the right orthogonal one.

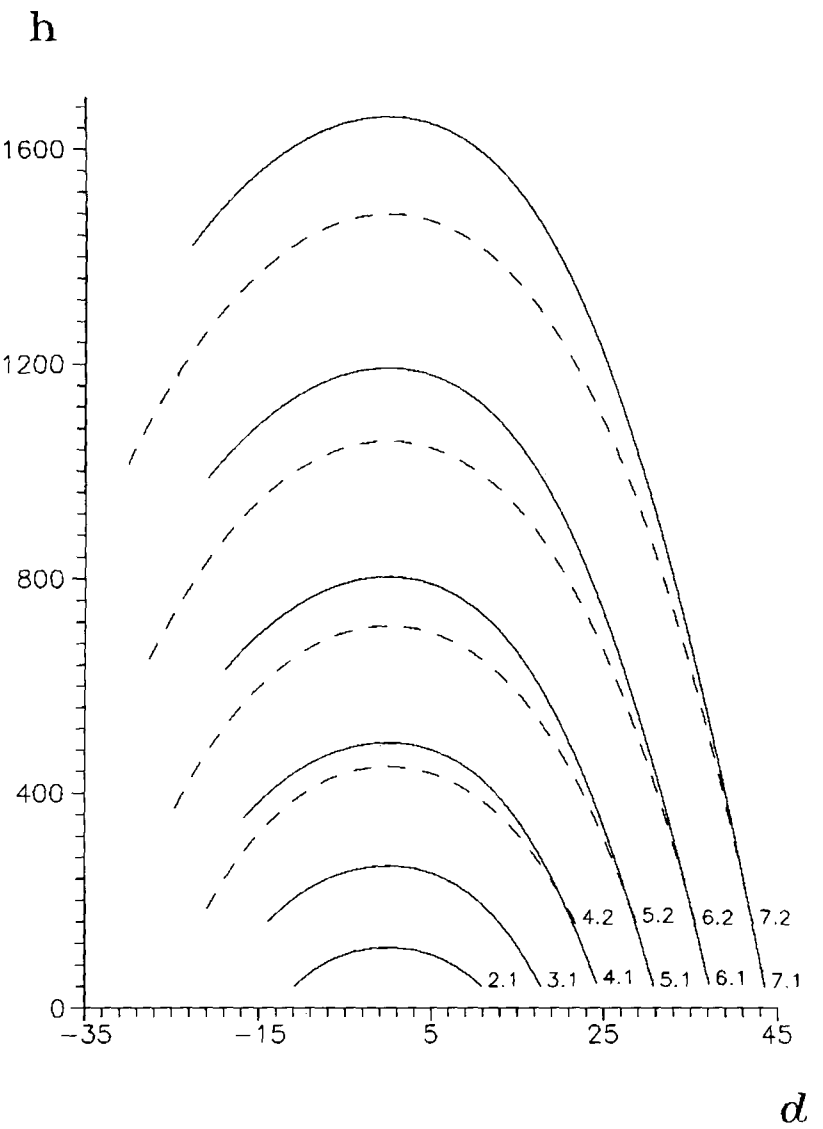

Figure 8. The normalized bending energy density $h(d)$ for closed equilibria. The curves are marked with two numbers: the first indicates m_0, the second – m_1 (its value is given for starting non-perturbed solutions). Two series of conformations are presented for $m_1 = 1$ and $m_1 = 2$.

Rewriting Equations (2) in the principal axes of bending and twisting gives

$$\mathbf{F}^* + \omega \times \mathbf{F} - \mathbf{f} = 0, \qquad \mathbf{M}^* + \omega \times \mathbf{M} + \mathbf{m} - \tau \times \mathbf{F} = 0, \tag{3}$$

where $*$ denotes differentiation with respect to s in the local coordinate system, ω is the Darboux vector for the rod in the deformed state.

Further, the case will be considered when the rod is deformed by the forces and moments at its ends only. Denote by γ the unit vector in the direction of the end force $\mathbf{F} = P\gamma$. The

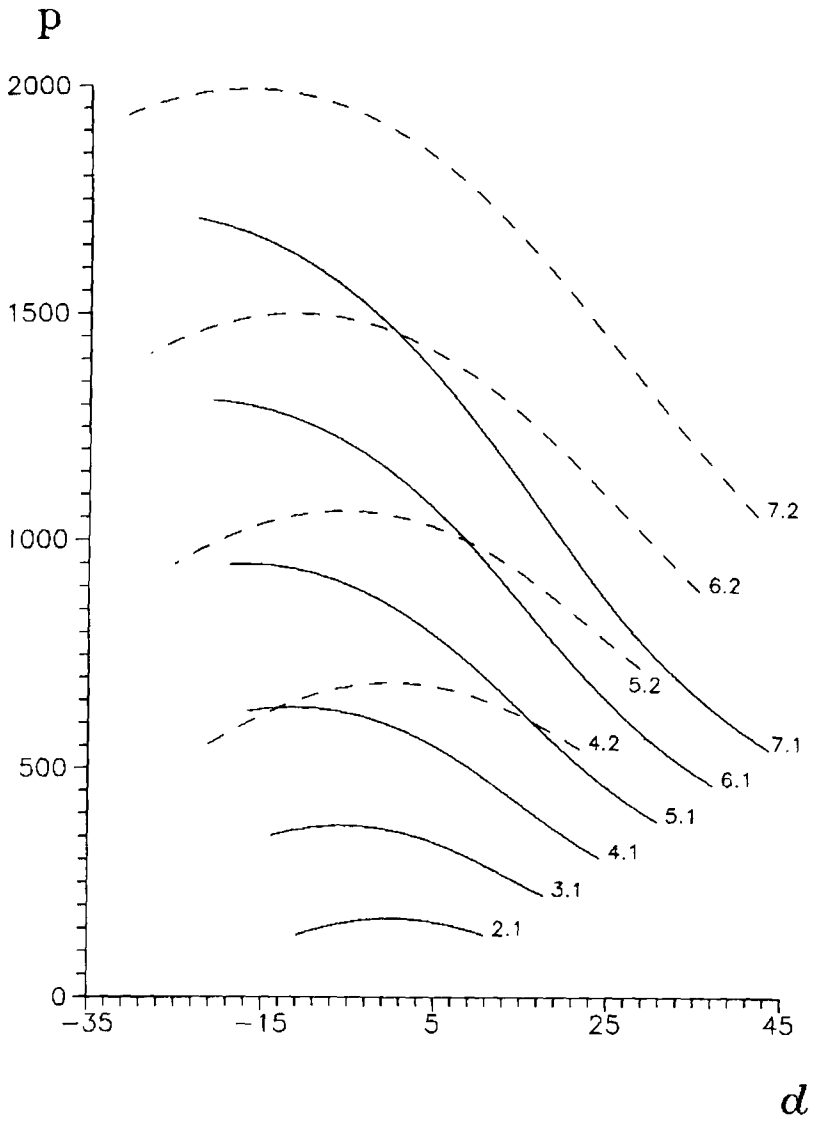

Figure 9. The normalized end force $p(d)$ for closed equilibria. The curves are marked with two numbers: the first indicates m_0, the second – m_1 (its value is given for starting non-perturbed solutions). Two series of conformations are presented for $m_1 = 1$ and $m_1 = 2$.

rod is assumed to be initially straight and not twisted. Then the second equation (3) takes the form

$$\mathbf{M}^* + \omega \times \mathbf{M} = P\,\tau \times \gamma. \tag{4}$$

The following kinematic equation is to be added to it:

$$\gamma^* = \gamma \times \omega. \tag{5}$$

According to the Hooke generalized law, the relationships that complete the system of equations may be written in the form

$$\mathbf{M} = \mathrm{B}\omega,$$

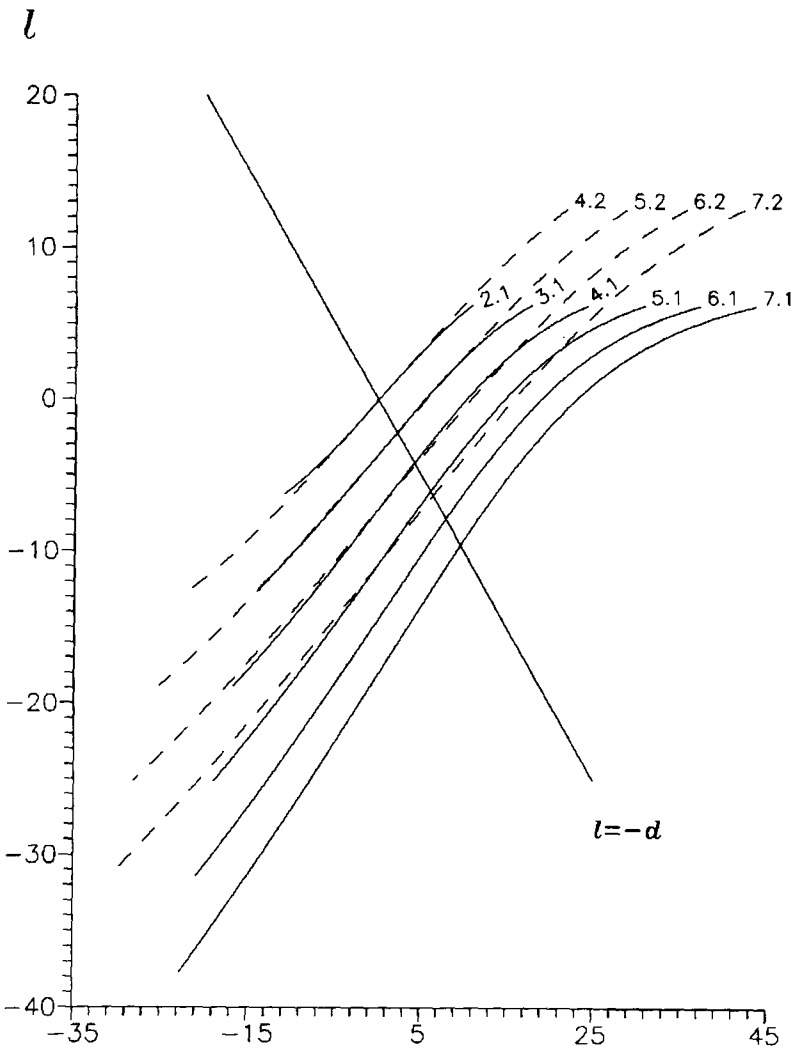

Figure 10. The normalized end moment $l(d)$ for closed equilibria. The curves are marked with two numbers: the first indicates m_0, the second m_1 (its value is given for starting non-perturbed solutions). Two series of conformations are presented for $m_1 = 1$ and $m_1 = 2$. The cross points of the curves with the bisectrix $l = -d$ correspond to the jump discontinuities of the function $\Phi(d)$.

where $\mathbf{B}$ is the stiffness matrix of the rod.

Consider the case of an initially curved and/or twisted rod. Let ω_0 be the Darboux vector for the rod in the relaxed state. Then Equation (4) is replaced by

$$(\mathbf{M} + \boldsymbol{\lambda})^* + \omega \times (\mathbf{M} + \boldsymbol{\lambda}) = P\,\tau \times \gamma. \tag{6}$$

The vector $\boldsymbol{\lambda}$ is determined by

$$\boldsymbol{\lambda} = -\mathbf{B}\omega_0.$$

The system of equations (6), (5) allows for three invariants:

$$\|\gamma\| = 1$$

(the geometrical identity),

$$(\mathbf{M} + \boldsymbol{\lambda}) \cdot \gamma = L, \tag{7}$$

which means that the projection of the moment $\mathbf{M} + \boldsymbol{\lambda}$ on the direction of the end force (the end moment value) is constant L, and

$$\mathbf{M} \cdot \boldsymbol{\omega} - 2P\gamma \cdot \boldsymbol{\tau} = 2H, \tag{8}$$

where H has the sense of the elastic energy density along the rod.

Thus, the problem of the curved and twisted elastic rod is described by the equations that formally coincide with the equations of a heavy gyrostat [11]. If the rod is initially straight and not twisted then its equations are analogous to those governing the motion of the heavy rigid body about a fixed point in the Lagrange case (the Kirchhoff analogy). The invariants (7) and (8) are analogs of the integral of angular momentum and the integral of energy in the problem of rigid body rotation about a fixed point. The difference from the rigid body or the gyrostat is in conditions which the components of the matrix $\mathbf{B}$ have to satisfy.

Now assume that the cross section is coincident with the elastic symmetry plane of the rod ($B_{ij} = 0, i \neq j$) and the principal bending stiffness coefficients are equal ($B_{22} = B_{33}$).

Assume next that the rod is initially straight: $\omega_2^0 = \omega_3^0 = 0$, but it may be twisted with some ω_1^0, as it takes place for the DNA molecule.

Taking into account the above assumptions, write Equations (6) in the coordinate form in the principal axes of bending and twisting:

$$\begin{aligned}
B_{11}\frac{\mathrm{d}\omega_1}{\mathrm{d}s} &= 0,\\
B_{22}\frac{\mathrm{d}\omega_2}{\mathrm{d}s} + B_{11}\omega_3(\omega_1 - \omega_1^0) - B_{22}\omega_1\omega_3 + P\bar{\bar{\gamma}} &= 0,\\
B_{22}\frac{\mathrm{d}\omega_3}{\mathrm{d}s} + B_{22}\omega_1\omega_2 - B_{11}\omega_2(\omega_1 - \omega_1^0) - P\bar{\gamma} &= 0,
\end{aligned} \tag{9}$$

where $\gamma = (\gamma, \bar{\gamma}, \bar{\bar{\gamma}})^{\mathsf{T}}$, $^{\mathsf{T}}$ denotes the transpose.

Clearly, it is assumed that always $B_{11} \neq 0, B_{22} = B_{33} \neq 0$.

The first Equation (9) implies immediately

$$\omega_1 = \omega_1^* = \text{const}. \tag{10}$$

This means that the twisting rate of the rod in the stressed state is constant along the rod. However, it is not necessary to be equal to the initial value in the relaxed state.

By introducing parameters $b = \frac{B_{11}}{B_{22}}$ and $p = \frac{-2P}{B_{22}}$ rewrite the two remained Equations (9) in the dimensionless form

$$\frac{\mathrm{d}\omega_2}{\mathrm{d}s} + \omega_3\left((b-1)\omega_1^* - b\omega_1^0\right) - \frac{p}{2}\bar{\bar{\gamma}} = 0, \qquad \frac{\mathrm{d}\omega_3}{\mathrm{d}s} - \omega_2\left((b-1)\omega_1^* - b\omega_1^0\right) + \frac{p}{2}\bar{\gamma} = 0.$$

Correspondingly, the integrals (7) and (8) transform to

$$b(\omega_1^* - \omega_1^0)\gamma + \omega_2\bar{\gamma} + \omega_3\bar{\bar{\gamma}} = l, \tag{11}$$

$l = \dfrac{L}{B_{22}}$, and to

$$\omega_2^2 + \omega_3^2 + p\gamma = h, \tag{12}$$

$$h = \frac{(2H - B_{11}\omega_1^{*2})}{B_{22}}.$$

The parameters p and l are the normalized end force and end moment values, respectively.

The parameter h is a characteristic of the normalized bending component of the strain energy density, which is to be constant along the rod.

3.2. Solution of the Equations. The Shape of the Central Axis

The forces applied to the rod end that corresponds to the initial value of the arc coordinate s can be brought to the central line. Introduce a coordinate system $\xi_1\xi_2\xi_3$ fixed in space and align axis ξ_1 with the direction of the end force $P\gamma$.

The attitude of the principal axes of bending and twisting $x_1x_2x_3$ with respect to the coordinate system $\xi_1\xi_2\xi_3$ is given by the three Euler angles ψ, φ, ϑ (Figure 4). Hence,

$$\begin{aligned} \gamma &= \cos\vartheta, \\ \overline{\gamma} &= \sin\vartheta\sin\varphi, \\ \overline{\overline{\gamma}} &= \sin\vartheta\cos\varphi. \end{aligned} \tag{13}$$

The vector ω specifies the angular velocity of rotation of the axes $x_1x_2x_3$ with respect to the fixed coordinate system. An analog of the Euler kinematic equations is valid

$$\begin{aligned} \omega_1 &= \frac{\mathrm{d}\varphi}{\mathrm{d}s} + \frac{\mathrm{d}\psi}{\mathrm{d}s}\cos\vartheta, \\ \omega_2 &= \frac{\mathrm{d}\psi}{\mathrm{d}s}\sin\vartheta\sin\varphi + \frac{\mathrm{d}\vartheta}{\mathrm{d}s}\cos\varphi, \\ \omega_3 &= \frac{\mathrm{d}\psi}{\mathrm{d}s}\sin\vartheta\cos\varphi - \frac{\mathrm{d}\vartheta}{\mathrm{d}s}\sin\varphi. \end{aligned} \tag{14}$$

The integrals (11) and (12) can be written, in view of (13) and (14), as

$$\gamma d + (1 - \gamma^2)\frac{\mathrm{d}\psi}{\mathrm{d}s} = l, \tag{15}$$

where $d = b(\omega_1^* - \omega_1^0)$, and

$$(1 - \gamma^2)\left(\frac{\mathrm{d}\psi}{\mathrm{d}s}\right)^2 + \left(\frac{\mathrm{d}\vartheta}{\mathrm{d}s}\right)^2 + \gamma p = h, \tag{16}$$

respectively.

The parameter d is proportional to the difference between twisting numbers in the relaxed and stressed states. It also depends on the Poisson ratio of the rod.

By eliminating the derivative $\frac{\mathrm{d}\psi}{\mathrm{d}s}$ from (15) and (16) and using the first formula of (13), a differential equation for γ can be obtained:

$$\left(\frac{\mathrm{d}\gamma}{\mathrm{d}s}\right)^2 = f(\gamma), \tag{17}$$

where $f(\gamma) = (h - p\gamma)(1 - \gamma^2) - (l - \mathrm{d}\gamma)^2$.

Clearly, $f(\pm 1) \leq 0$.

Without loss of generality, it may be thought that $p > 0$ (if $p = 0$ then this is an analog of the Euler–Poinsot case of the motion of the rigid body with a spheroid as the inertia ellipsoid; it can be shown that then no non-trivial closed configurations exist [6] in this case). For $p > 0$, the function $f \to +\infty$ as $\gamma \to +\infty$. Therefore, the cubic polynomial $f(\gamma)$ has at least one real root $\gamma_3 > 1$. By the first equation of (13), only the interval $|\gamma| \leq 1$ is of interest. Since $\left(\frac{d\gamma}{ds}\right)^2$ must be non-negative for real solutions, the polynomial $f(\gamma)$ must have two real roots in this interval: $-1 \leq \gamma_1 \leq \gamma_2 \leq 1$.

Bring Equation (17) to the form

$$\left(\frac{d\gamma}{ds}\right)^2 = p(\gamma - \gamma_1)(\gamma - \gamma_2)(\gamma - \gamma_3). \tag{18}$$

By introducing a new variable v given by

$$\gamma = \gamma_1 + (\gamma_2 - \gamma_1)v^2,$$

Equation (18) may be recast to

$$\left(\frac{dv}{ds}\right)^2 = \Omega^2(1 - v^2)(1 - kv^2), \tag{19}$$

where $\Omega^2 = \frac{p}{4}(\gamma_3 - \gamma_1), \Omega > 0$, and $k^2 = \frac{\gamma_2 - \gamma_1}{\gamma_3 - \gamma_1}, 0 \leq k \leq 1$.

Integration of Equation (19) leads to

$$\mathrm{F}(v, k) = \Omega(s - s_0), \tag{20}$$

where $\mathrm{F}(v, k)$ is the elliptic integral of the first kind of the modulus k:

$$\mathrm{F}(v, k) = \int_0^v \frac{d\overline{v}}{\sqrt{(1 - \overline{v}^2)(1 - k^2\overline{v}^2)}}.$$

Equation (20) has the solution $v = \mathrm{sn}\,\Omega(s - s_0)$, which gives for γ

$$\gamma = \gamma_1 + (\gamma_2 - \gamma_1)\,\mathrm{sn}^2\,\Omega(s - s_0). \tag{21}$$

The derivative $\frac{d\psi}{ds}$ can be obtained from Equation (15) as a function of γ. After some manipulations, the following equation is obtained

$$\frac{d\psi}{ds} = \frac{l - d}{2(1 - \gamma_1)} \frac{1}{1 - n_1\,\mathrm{sn}^2\,\Omega(s - s_0)} + \frac{l + d}{2(1 + \gamma_1)} \frac{1}{1 - n_2\,\mathrm{sn}^2\,\Omega(s - s_0)}, \tag{22}$$

where $n_1 = \frac{\gamma_1 - \gamma_2}{\gamma_1 - 1}, n_2 = \frac{\gamma_1 - \gamma_2}{\gamma_1 + 1}$.

Integration of Equation (22) yields

$$\psi - \psi_0 = \frac{l - d}{2(1 - \gamma_1)\Omega} \Pi\left(\mathrm{am}(\Omega(s - s_0)), n_1, k\right) + \frac{l + d}{2(1 + \gamma_1)\Omega} \Pi\left(\mathrm{am}(\Omega(s - s_0)), n_2, k\right),$$

where $\Pi(v, n, k)$ is the elliptic integral of the third kind:

$$\Pi(v, n, k) = \int_0^v \frac{\mathrm{d}\overline{v}}{(1 - n\overline{v}^2)\sqrt{(1 - \overline{v}^2)(1 - k^2\overline{v}^2)}}.$$

Now from the first Equation (14)

$$\frac{\mathrm{d}\varphi}{\mathrm{d}s} = \omega_1^* - \gamma\frac{\mathrm{d}\psi}{\mathrm{d}s},$$

which yields after integrating

$$\varphi - \varphi_0 = (\omega_1^* - d)(s - s_0) + \frac{d - l}{2(1 - \gamma_1)\Omega}\Pi\left(\mathrm{am}(\Omega(s - s_0)), n_1, k\right) + \frac{d + l}{2(1 + \gamma_1)\Omega}\Pi\left(\mathrm{am}(\Omega(s - s_0)), n_2, k\right).$$

Up to this point the consideration has been carried out within the framework of the traditional approach to investigation of the Lagrange top. However, a knowledge of the orientation of the principal axes of bending and twisting is not enough to determine the rod shape. Therefore, the equations by Ilyukhin [20] will be used for the cylindrical coordinates ρ, α, ζ of the central axis of the rod (Figure 5)

$$\rho^2 = \frac{1}{P^2}M_\rho^2, \tag{23}$$

$$\frac{\mathrm{d}\alpha}{\mathrm{d}s} = P\frac{L\gamma - (M_1 + \lambda_1)}{M_\rho^2}, \tag{24}$$

$$\frac{\mathrm{d}\zeta}{\mathrm{d}s} = \gamma, \tag{25}$$

where $M_\rho^2 = \|\mathbf{M} + \boldsymbol{\lambda}\|^2 - L^2$.

In the dimensionless form, Equation (23) appears as

$$\rho = \frac{2\sqrt{d^2 - l^2 + h - p\gamma}}{p}, \tag{26}$$

and Equation (24) as

$$\frac{\mathrm{d}\alpha}{\mathrm{d}s} = -\frac{p(l\gamma - d)}{2(d^2 - l^2 + h - p\gamma)}. \tag{27}$$

By substituting the solution (21) into the last equation and integrating it, a formula for the angle α is obtained

$$\alpha - \alpha_0 = \frac{l}{2}(s - s_0) - \frac{l(d^2 - l^2 + h) - pd}{2\Omega(d^2 - l^2 + h - p\gamma_1)}\Pi\left(\mathrm{am}(\Omega(s - s_0)), n, k\right), \tag{28}$$

where $n = \dfrac{p(\gamma_2 - \gamma_1)}{d^2 - l^2 + h - p\gamma_1}$.

Finally, after substituting (21) and integrating, the third coordinate ζ can be found from (25)

$$\zeta - \zeta_0 = \gamma_3(s - s_0) - 2\sqrt{\frac{\gamma_3 - \gamma_1}{p}}\,\mathrm{E}\left(\mathrm{am}(\Omega(s - s_0)), k\right), \tag{29}$$

where $\mathrm{E}(v, k)$ is the elliptic integral of the second kind of the modulus k:

$$\mathrm{E}(v, k) = \int_0^v \sqrt{\frac{1 - k^2\overline{v}^2}{1 - \overline{v}^2}}\,d\overline{v}.$$

The following formula [21] was used to derive (29):

$$\int \mathrm{sn}^2\, u\, \mathrm{d}u = \frac{1}{k^2}\left(u - \mathrm{E}(\mathrm{am}\, u, k)\right).$$

The three Equations (26), (28), and (29) determine entirely the shape of the central axis of the rod.

3.3. Equilibrium Equations of a Closed Molecule of DNA

Now a problem is set to find an equilibrium shape of the looped DNA molecule. The model rod is supposed to be straight and possibly twisted in the relaxed state when its ends are not closed. We assume that no external forces or moments act on the molecule.

The problem statement requires that the model elastic rod is smoothly closed into a circle. By this is meant that its ends coincide with each other and an orientation of the principal axes of bending and twisting and the Darboux vector are the same at the both ends. Without loss of generality, the rod length may be put $S = 1$ and $s_0 = 0$. The corresponding boundary value problem results in

$$\rho\,|_0 = \rho\,|_1, \qquad \alpha\,|_0 = \alpha\,|_1\,(\mathrm{mod}\,2\pi), \qquad \zeta\,|_0 = \zeta\,|_1,$$

$$\vartheta\,|_0 = \vartheta\,|_1\,(\mathrm{mod}\,2\pi), \qquad \psi\,|_0 = \psi\,|_1\,(\mathrm{mod}\,2\pi), \qquad \varphi\,|_0 = \varphi\,|_1\,(\mathrm{mod}\,2\pi), \tag{30}$$

$$\omega_i\,|_0 = \omega_i\,|_1, \quad i = 1, 2, 3. \tag{31}$$

Notice that the integrals (10), (15), (16) and Equations (14) imply immediately that the last conditions (31) are fulfilled automatically, if the conditions (30) are satisfied.

We choose $\Omega = 2m_0\,\mathrm{K}(k)$, where $m_0 = 1, 2, \ldots$, and $K(k) = \mathrm{F}\left(\frac{\pi}{2}, k\right)$ is the complete elliptic integral of the first kind of the modulus k. Then, as it can be readily seen from solution (21) and from (26), the periodicity conditions for ϑ and ρ are met. Moreover, in this event the tangent vectors to the central axis of the rod have the same direction — this follows from the view of the right sides of (26), (28), (29). Therefore, only the last condition from (30) is enough to remain.

Thus, in order to solve the above formulated problem it is necessary to find such values of the parameters h, p, l and ω_1^* that satisfy the system of four nonlinear equations:

$$\Omega = 2m_0\,\mathrm{K}(k), \qquad m_0 = 1, 2, \ldots, \tag{32}$$

$$l\,\mathrm{K}(k) - \frac{l(d^2 - l^2 + h) - pd}{d^2 - l^2 + h - p\gamma_1}\,\Pi(n, k) = 4\pi m_1\,\mathrm{K}(k), \qquad m_1 = 0, \pm 1, \pm 2, \ldots, \tag{33}$$

$$\gamma_3\,\mathrm{K}(k) - (\gamma_3 - \gamma_1)\,\mathrm{E}(k) = 0, \tag{34}$$

$$\frac{l-d}{\gamma_1-1}\,\Pi(n_1,k)+\frac{l+d}{\gamma_1+1}\,\Pi(n_2,k)=2\,\mathrm{K}(k)\,(2\pi m_2+(d-\omega_1^*))\,,$$
$$m_2=0,\pm1,\pm2,\ldots, \qquad (35)$$

where $\mathrm{E}(k)=\mathrm{E}(\frac{\pi}{2},k)$, $\Pi(n,k)=\Pi(\frac{\pi}{2},n,k)$ are the complete elliptic integrals of the second and third kind, respectively.

Equation (33) corresponds to the periodicity condition in α, Equation (34) – in ζ, and Equation (35) – in φ. Equations (32)–(34) determine the shape of the central axis of the molecule (hence, its writhing number), while Equation (35) corresponds to the proper closure of the chains of complementary nucleotides (hence, its solutions correlate with the twisting number).

The four Equations (32), (33), (34), and (35) contain three arbitrary integers m_0, m_1, and m_2. Giving various values to them one can take different solutions. The integer m_1 counts the number of turns around the fixed axis ξ_1 and the integer m_0 is the number of supercoils. The integer m_2 is responsible for the twist.

It is convenient for the following to represent Equation (35) in the form

$$\Phi(d)=\omega_1^0+\sigma d, \qquad (36)$$

where

$$\Phi(d)=\frac{1}{2\,\mathrm{K}(k)}\left(\frac{l-d}{1-\gamma_1}\Pi(n_1,k)-\frac{l+d}{1+\gamma_1}\Pi(n_2,k)\right)+2\pi m_2. \qquad (37)$$

The function $\Phi(d)$ may be considered as a function of d on the assumption that the three other unknowns (i. e., h, p, and l) are chosen to satisfy the first three Equations (32)–(34).

In addition to h, p, l and ω_1^*, two more parameters appear in Equations (32)–(35): $b=\frac{1}{\sigma+1}$ (recall that the Poisson ratio σ is a characteristic of the elastic properties of the molecule) and ω_1^0, which is, within a constant factor, the twisting of the molecule in the relaxed state: $Tw_0=\frac{\omega_1^0}{2\pi}$. Instead of the parameter ω_1^*, which determines the twisting in the stressed state: $Tw=\frac{\omega_1^*}{2\pi}$, it is convenient to take $d=b(\omega_1^*-\omega_1^0)$ as an independent parameter.

Discontinuity of the function $\Phi(d)$. For $l=-d$ the polynomial $f(\gamma)$ in (17) has the root $\gamma_1=-1$ and the second summand in (37) is indeterminate. Consider the vicinity of this point by letting $l=-d+\epsilon$ with $|\,\epsilon\,|\ll 1$. Then it may be shown that

$$\gamma_1=-1+\frac{\epsilon^2}{2(h+p)}+O(\epsilon^3),$$
$$\gamma_{2,3}=\frac{p+h+d^2\mp\sqrt{(p+h+d^2)^2-4p(h-d^2)}}{2p}+O(\epsilon) \qquad (38)$$

and the parameter n_2 allows for the following approximation:

$$n_2=-2(h+p)(1+\gamma_2)\epsilon^{-2}+O(1),$$

$n_2<0$ since $\gamma_2>\gamma_1$.

Now the integral $\Pi(n_2,k)$ may be estimated by using the formula

$$\Pi(n,k)=\frac{1}{1-n}\,\mathrm{K}(k)+$$

$$\sqrt{\frac{n}{(k^2-n)(n-1)}}\left(\frac{\pi}{2}+(\mathrm{K}(k)-\mathrm{E}(k))\,\mathrm{F}(\epsilon_N,k')-\mathrm{K}(k)\,\mathrm{E}(\epsilon_N,k')\right) \tag{39}$$

(see [21] for more formulas for elliptic integrals). Here, $\epsilon_N = \sin^{-1}(1-n)^{-\frac{1}{2}}$ and k' is the comodulus to k, $k^2+k'^2=1$.

In the case considered (39) gives

$$\Pi(n_2,k)=\frac{\pi}{2}\frac{|\epsilon|}{\sqrt{2(h+p)(1+\gamma_2)}}+O(\epsilon^2).$$

Now the second summand in (37) may be estimated

$$-\frac{1}{2\,\mathrm{K}(k)}\frac{l+d}{1+\gamma_1}\Pi(n_2,k)=-\frac{\pi}{2\,\mathrm{K}(k)}\sqrt{\frac{h+p}{2(1+\gamma_2)}}\operatorname{sign}\epsilon+O(\epsilon). \tag{40}$$

Therefore, the function $\Phi(d)$ has a finite discontinuity at $d=-l$ if m_2 is constant. After some manipulation the jump value $\Delta\Phi$ can be obtained by using (32), (38) and (40)

$$\Delta\Phi = 2\pi m_0. \tag{41}$$

It follows from (27) that for $d=-l$ the projection of the central axis on the plane $\xi\eta$ has cusp points for $\gamma=\gamma_1$. For $d>-l$ this curve has loops and $\alpha(s)$ is monotonic when $d<-l$.

Since the function $\Phi(d)$ is defined with a precision of $2\pi m_2$ in (37), its jumps may be compensated by an appropriate change of m_2.

3.4. Plane Solutions

Before proceeding to general spatial configurations of the rod, consider two exact plane solutions of the above BVP (32)–(35) [8].

Plane ring. Let Equation (17) have a solution $\gamma\equiv 0$, then

$$\gamma_1=\gamma_2=0,\qquad \gamma_3=\frac{l^2+d^2}{2ld}>1.$$

The parameters have to satisfy the relationships

$$h=l^2,\qquad p=2ld.$$

Equation (25) implies $\zeta=\zeta_0=$ const, Equation (26) — $\rho=\frac{1}{|l|}$, and Equation (27) — $\alpha=ls+\alpha_0$. By integrating Equation (15) obtain $\psi=ls+\psi_0$. Finally, from the Euler first kinematic equation (14), $\varphi=\omega_1^* s+\varphi_0$. The periodicity conditions are satisfied if

$$l=2\pi m_1,\qquad m_1=\pm1,\pm2,\ldots,$$

and

$$\omega_1^*=2\pi m_2,\qquad m_2=0,\pm1,\pm2,\ldots.$$

Thus, the rod central axis is a plane circle of radius $\rho=\frac{1}{|l|}$, covered $|\,m_1\,|$ times.

8-figure shape. We search for a closed configuration with $l=0$, $d=0$. The condidion (33) is then met. Two cases are possible:

(1) $h < p$, $\gamma_1 = -1$, $\gamma_2 = \frac{h}{p}$, $\gamma_3 = 1$, $k^2 = \frac{1}{2}\left(\frac{h}{p} + 1\right)$. The condition (34) transforms into

$$\mathrm{K}(k) = 2\,\mathrm{E}(k),$$

which yields the modulus value $k \cong 0.9089$, and the parameters h and p have to satisfy the condition $h \cong 0.6522p$.

From (21)

$$\gamma = -1 + \left(\frac{h}{p} + 1\right) \mathrm{sn}^2\left(\frac{p}{\sqrt{2}}s\right),$$

and the condition (32) is

$$\frac{p}{\sqrt{2}} = 2m_0\,\mathrm{K}(k),$$

from which the value of p may be found.

(2) $h > p$, $\gamma_1 = -1$, $\gamma_2 = 1$, $\gamma_3 = \frac{h}{p}$, $k^2 = 2\left(\frac{h}{p} + 1\right)^{-1}$. The condition (34) transforms into

$$(2 - k^2)\,\mathrm{K}(k) = 2\,\mathrm{E}(k),$$

which has no solution.

3.5. Solutions with Self-intersections

The plane 8-figure has a self-intersection point. There may exist different non-planar solutions with self-intersection points. We search symmetrical solutions with self-crossings at the origin. Then for such points $\rho = 0$ and Equation (26) implies

$$d^2 - l^2 + h - p\gamma = 0 \quad \text{for} \quad \gamma = \gamma_2$$

since $p > 0$ and $\gamma_1 \leq \gamma \leq \gamma_2$. Then the parameter n introduced in (28) is $n = 1$ and $l\gamma_2 = d$. For $\gamma \neq \gamma_2$ the polar angle α is a linear function of s because the second term in (28) vanishes. When $\gamma = \gamma_2$, the solution passes through the origin and the angle α jumps by $\pm\pi$ (the sign corresponds to the sign of m_1). The length of the arc between intersection points is $\Delta s = \frac{1}{m_0}$ and the change of α is $\Delta\alpha = 2\pi\frac{m_1}{m_0}$. From (28) we have

$$\Delta\alpha = \frac{l}{2}\Delta s + \pi\,\mathrm{sign}\ m_1,$$

which gives the value of l

$$l = 2\pi(2m_1 - m_0\,\mathrm{sign}\ m_1). \tag{42}$$

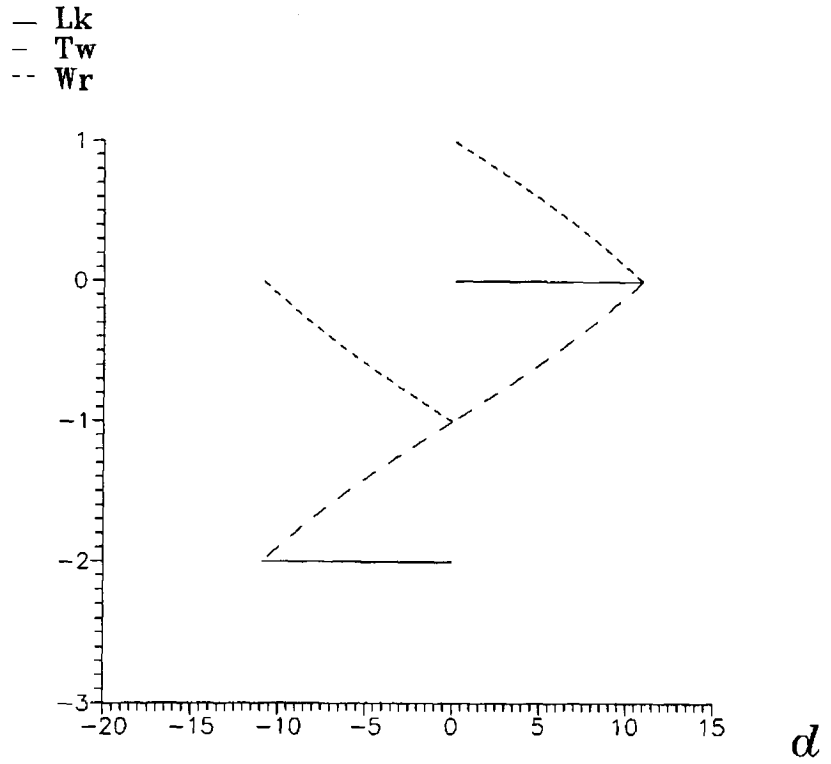

Figure 11. The linking, twisting and writhing numbers as functions of the parameter d for $m_0 = 2$.

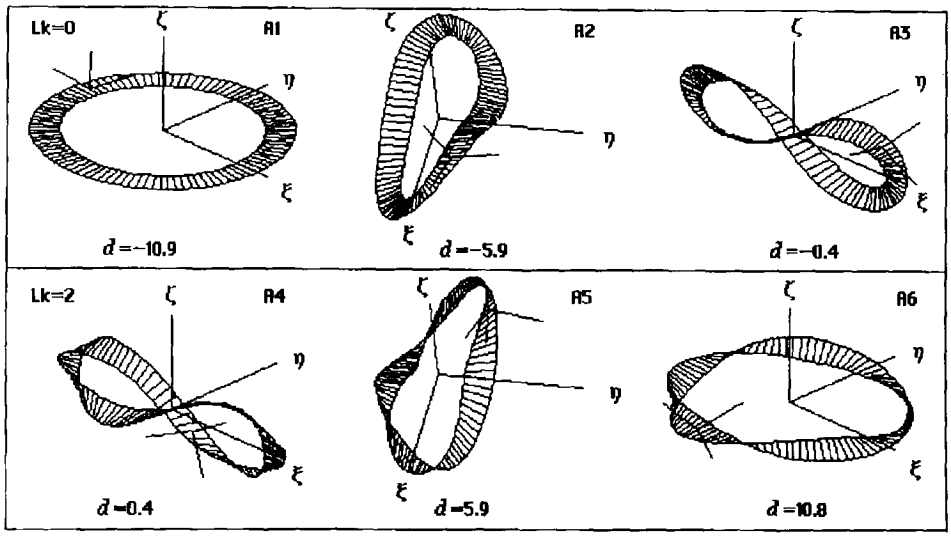

Figure 12. The shape transformation of the closed equlibria with change of the parameter d for $m_0 = 2$, A-sequence.

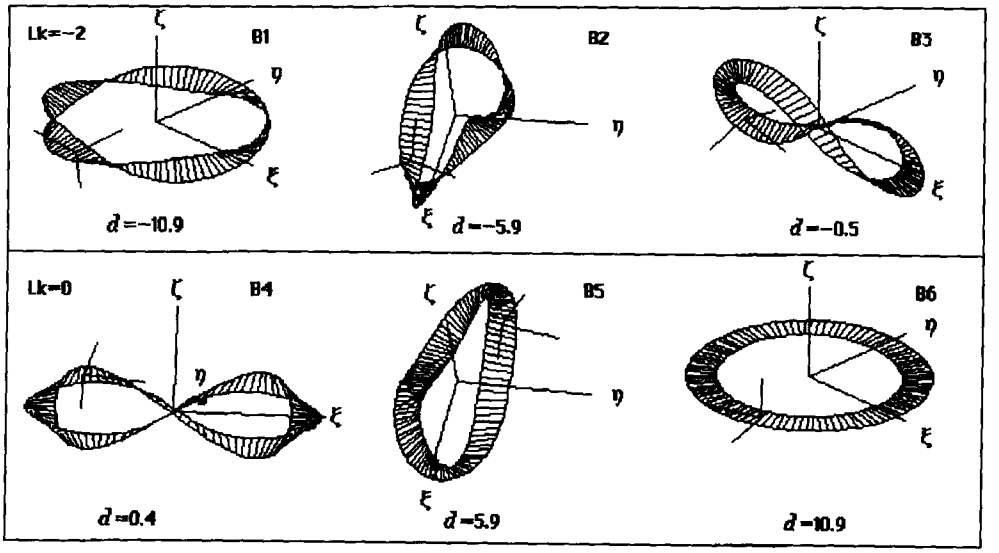

Figure 13. The shape transformation of the closed equlibria with change of the parameter d for $m_0 = 2$, B-sequence.

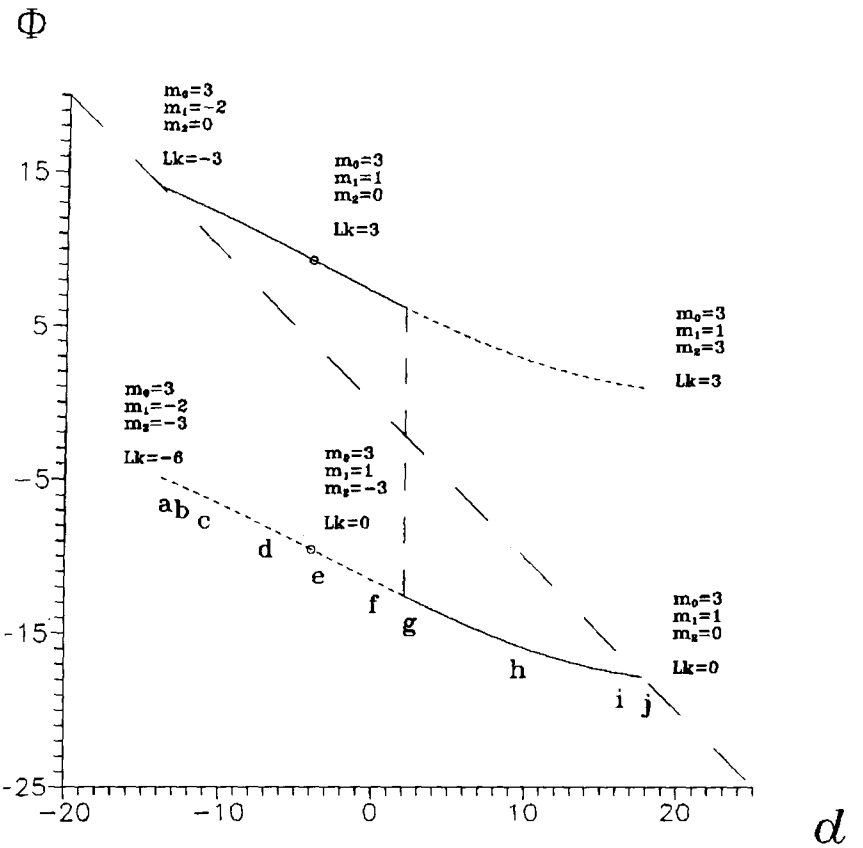

Figure 14. The function $\Phi(d)$ from (37) for $m_0 = 3$. Two branches are plotted. Small circles correspond to shapes with self-intersections.

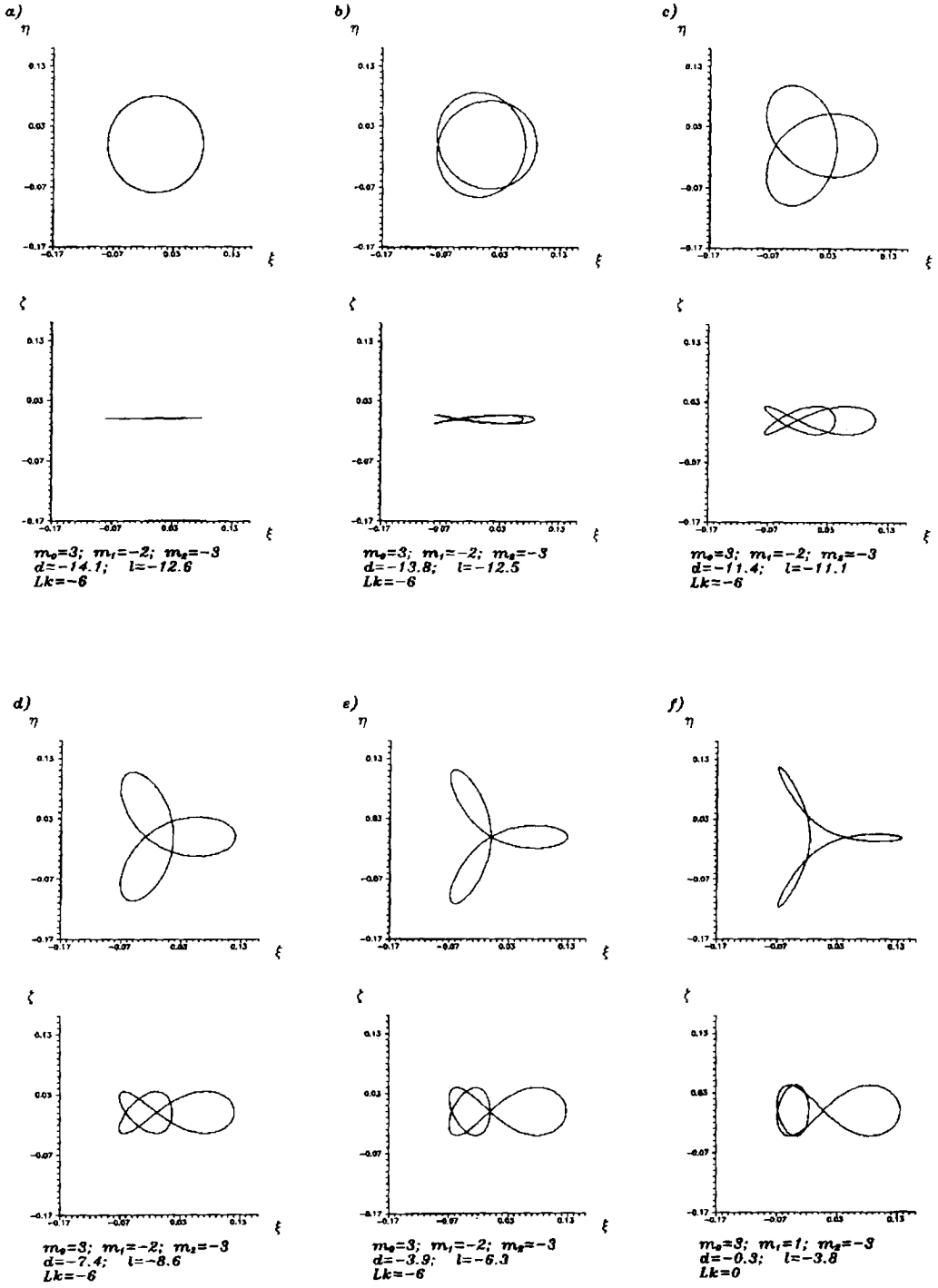

Figure 15. (cont.)

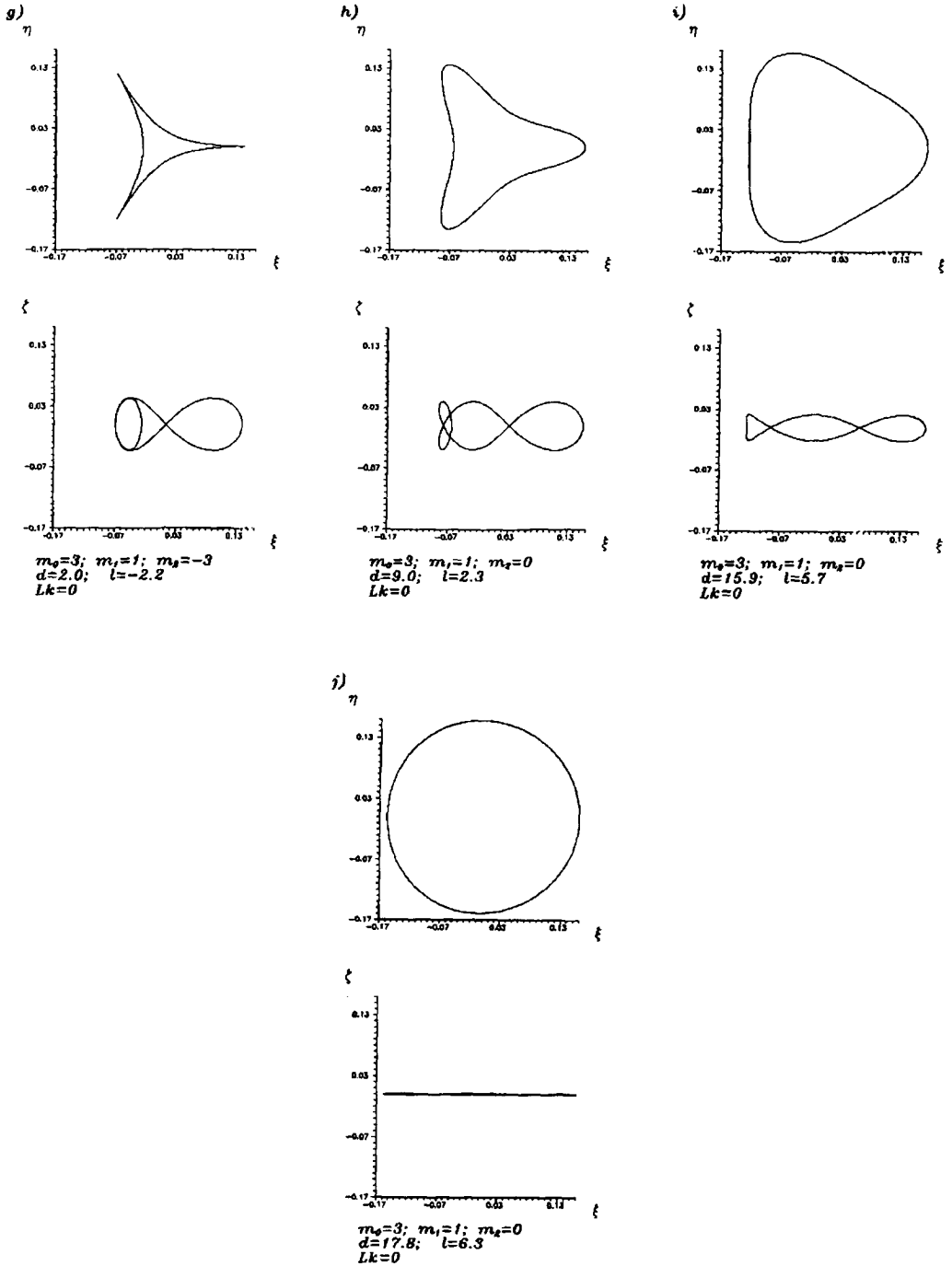

Figure 15. The projections of the central axis for various values of the parameter d for $m_0 = 3$.

3.6. Perturbation Analysis

In order to obtain nonplanar solutions of the system (32)–(35), a parameter continuation approach is proposed. The plane circular ring may be taken as a solution to be perturbed. The ring may be traced many times.

By using the perturbation analysis it is possible to find relations between the parameters of the ring for which periodic solutions are born.

Let

$$h = l^2 + \epsilon^2, \qquad p = 2ld + \beta\epsilon^2,$$

where $0 < \epsilon \ll 1$ and β is an unknown coefficient. We search for the approximate expressions for the roots of the equation $f(\gamma) = 0$ in the form

$$\gamma_{1,2} = \gamma_{11}\epsilon + O(\epsilon^2), \qquad \gamma_3 = \frac{l^2 + d^2}{2ld} + \gamma_{31}\epsilon + O(\epsilon^2).$$

Omitting some intermediate manipulations, the final expressions for coefficients is presented:

$$\gamma_{11} = (l^2 + d^2)^{-\frac{1}{2}}, \qquad \gamma_{31} = 0.$$

Obtain the expansions for the modulus k

$$k^2 = \frac{4ld}{(l^2 + d^2)^{\frac{3}{2}}}\epsilon + O(\epsilon^2), \tag{43}$$

and for the frequence

$$\Omega = \frac{1}{2}(l^2 + d^2)^{\frac{1}{2}} + \frac{ld}{2(l^2 + d^2)}\epsilon + O(\epsilon^2). \tag{44}$$

To expand the complete elliptic integrals K and E into the series use the formulas [21]:

$$\mathrm{K}(k) = \frac{\pi}{2}\left(1 + \frac{1^2}{2^2}k^2 + O(k^4)\right),$$

$$\mathrm{E}(k) = \frac{\pi}{2}\left(1 - \frac{1^2}{2^2}k^2 + O(k^4)\right).$$

Substituting (43) into the last formulas yields

$$\mathrm{K}(k) = \frac{\pi}{2} + \frac{\pi}{2}\frac{ld}{(l^2 + d^2)^{\frac{3}{2}}}\epsilon + O(\epsilon^2), \tag{45}$$

$$\mathrm{E}(k) = \frac{\pi}{2} - \frac{\pi}{2}\frac{ld}{(l^2 + d^2)^{\frac{3}{2}}}\epsilon + O(\epsilon^2).$$

Now insert the expansions (44) and (45) into the periodicity condition (32). By equating the coefficients by the powers ϵ^0 and ϵ^1 an equation is obtained for the parameters l and d:

$$\pm(l^2 + d^2)^{\frac{1}{2}} = 2\pi m_0. \tag{46}$$

It is easy to check that the condition (34) is satisfied, at least correct to the terms linear in ϵ.

The expansion of the parameter n may be obtained

$$n = \frac{4l}{d(l^2 + d^2)^{\frac{1}{2}}}\epsilon + O(\epsilon^2).$$

Then the following expression is valid for $\Pi(n, k)$:

$$\Pi(n, k) = \frac{\pi}{2} + \frac{\pi}{2}\frac{l(2l^2 + 3d^2)}{d(l^2 + d^2)^{\frac{3}{2}}}\epsilon + O(\epsilon^2). \tag{47}$$

Substitute the expansions (47) and (45) into the condition (33), equate the coefficients by the powers ϵ^0 and ϵ^1 and take into account (46). Then (33) is satisfied if the parameter l takes the following values:

$$l = 2\pi m_1, \qquad m_1 = 0, \pm 1, \pm 2, \ldots . \tag{48}$$

By using (48) the formula for d may be obtained from (46)

$$d = \pm 2\pi(m_0^2 - m_1^2)^{\frac{1}{2}}, \tag{49}$$

which implies $\mid m_0 \mid \geq \mid m_1 \mid$.

Thus, the quantized values are found which the parameters l and d must take to provide a possible birth of a non-planar solution.

3.7. The Spatial Shape of the Closed Molecule of DNA

The numerical procedure is implemented as follows. The parameter d is taken as a continuation parameter. Continuous change of the parameter d may be interpreted either as the natural twist variation for the DNA in solution, or as the variation of the elastic properties of the molecule (hence, the Poisson ratio). Both cases are experimentally accessible. Experimentally, it is found that the ethidium bromide affects the natural twist of the looped DNA [3].

Having chosen a set of the integers m_0, m_1, and m_2, the starting values of the parameters are calculated according to the above formulas: l and d are from (48) and (49), respectively, and $h = l^2, p = 2ld$. Then the value of d is made slightly different and the system (32)–(34) is solved by the Newton iteration with respect to h, p, and l. These three equations completely determine the shape of the central axis, and, hence, the writhing value. Now the function $\Phi(d)$ may be evaluated and substituted into (36), from where the initial twisting ω_1^0 is easily evaluated.

Figure 6 explains how this is carried out. Only two curves for $m_0 = 2$ are plotted. They are shifted by 4π from each other along the ordinate axis. The curves $\Phi(d)$ represent the left side of Equation (36). Intersections of them with a linear function of d in the right side give roots. In the case presented, there are two, marked d_1 and d_2. Having known their values one can easily find the twisting:

$$Tw_{1,2} = \frac{d_{1,2}}{2\pi b} + Tw_0,$$

where $Tw_0 = 2\pi\omega_1^0$ is the initial twisting.

Now consider concrete examples of solutions in more detail.

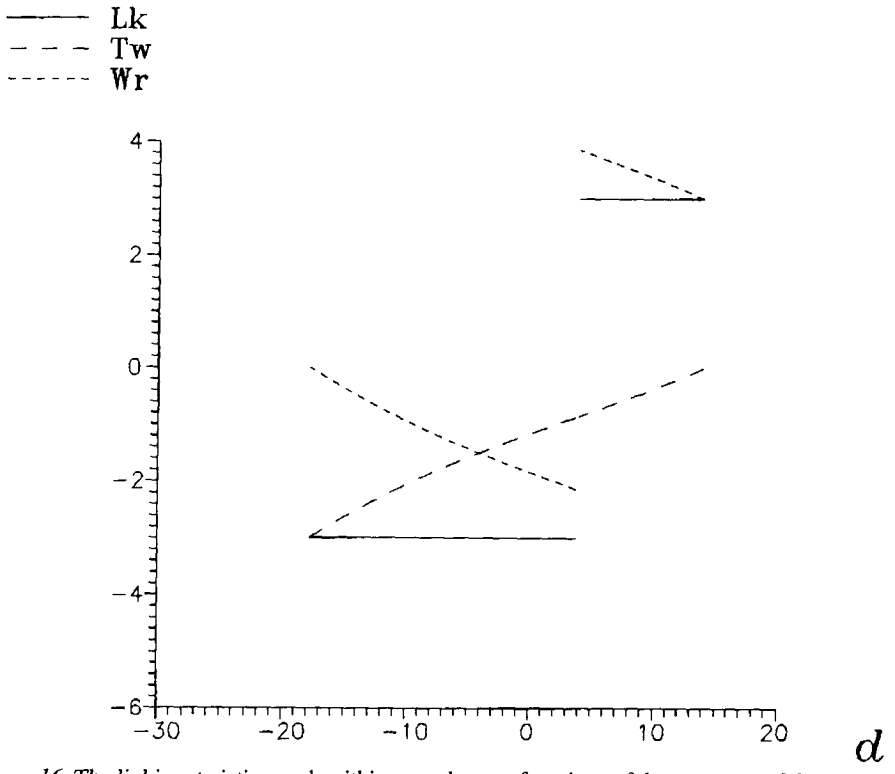

Figure 16. The linking, twisting and writhing numbers as functions of the parameter d for $m_0 = 3$.

Figures 7–10 show the graphs of the functions $\Phi(d)$, $h(d)$, $p(d)$, and $l(d)$, respectively. The curves are marked with two numbers: the first indicates m_0, the second — m_1 (its value is given for starting non-perturbed solutions). Two series of closed conformations are presented for $m_1 = 1$ and $m_1 = 2$. All the curves $\Phi(d)$ are shown continuous on the graphs since the number m_2 was just changed appropriately at $l = -d$. The displacement by $2\pi m_2$ gives infinite number of the branches of $\Phi(d)$.

$m_0 = 2$. This is the simplest case of non-planar conformations. To begin with there is the plane ring marked A1 in Figure 6:

$$l = -2\pi, \qquad d = -2\pi\sqrt{3}, \qquad h = 4\pi^2, \qquad p = 8\pi^2\sqrt{3} \qquad (m_0 = 2,\ m_1 = -1).$$

Then the function $\Phi(d)$ takes the form:

$$\Phi(d) = d + 2\pi m_2.$$

B1 is another example of the plane ring with the same parameters, but with different twist.

As the parameter d increases, the molecule begins to writhe (A2) until it forms the 8-figure at $d = 0$, $l = 0$ (A3). At this moment, the self-intersection must occur. However, the model under consideration allows for self-penetration of the molecule. At a single self-intersection only the topological invariant Lk changes from 0 to 2 (Figure 11) and the central axis shape deforms but little. From the basic relationship (1) it follows then that the writhing number must also change two. We can follow the same branch of the curve $\Phi(d)$ and observe configurations A4 to A6 with $Lk = 2$. Alternatively, the linking number may be fixed $Lk = 0$ and the switch

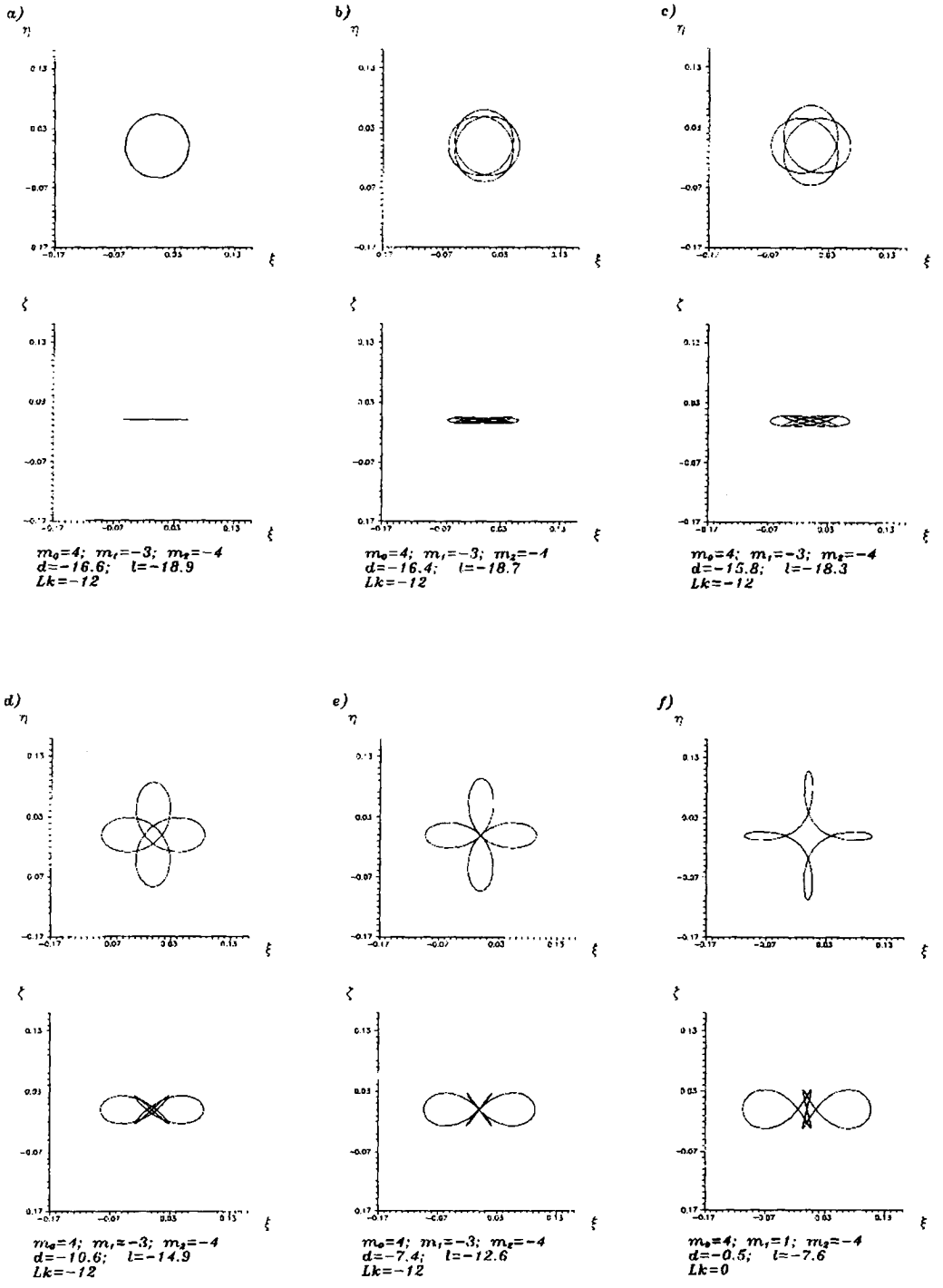

Figure 17. (cont.)

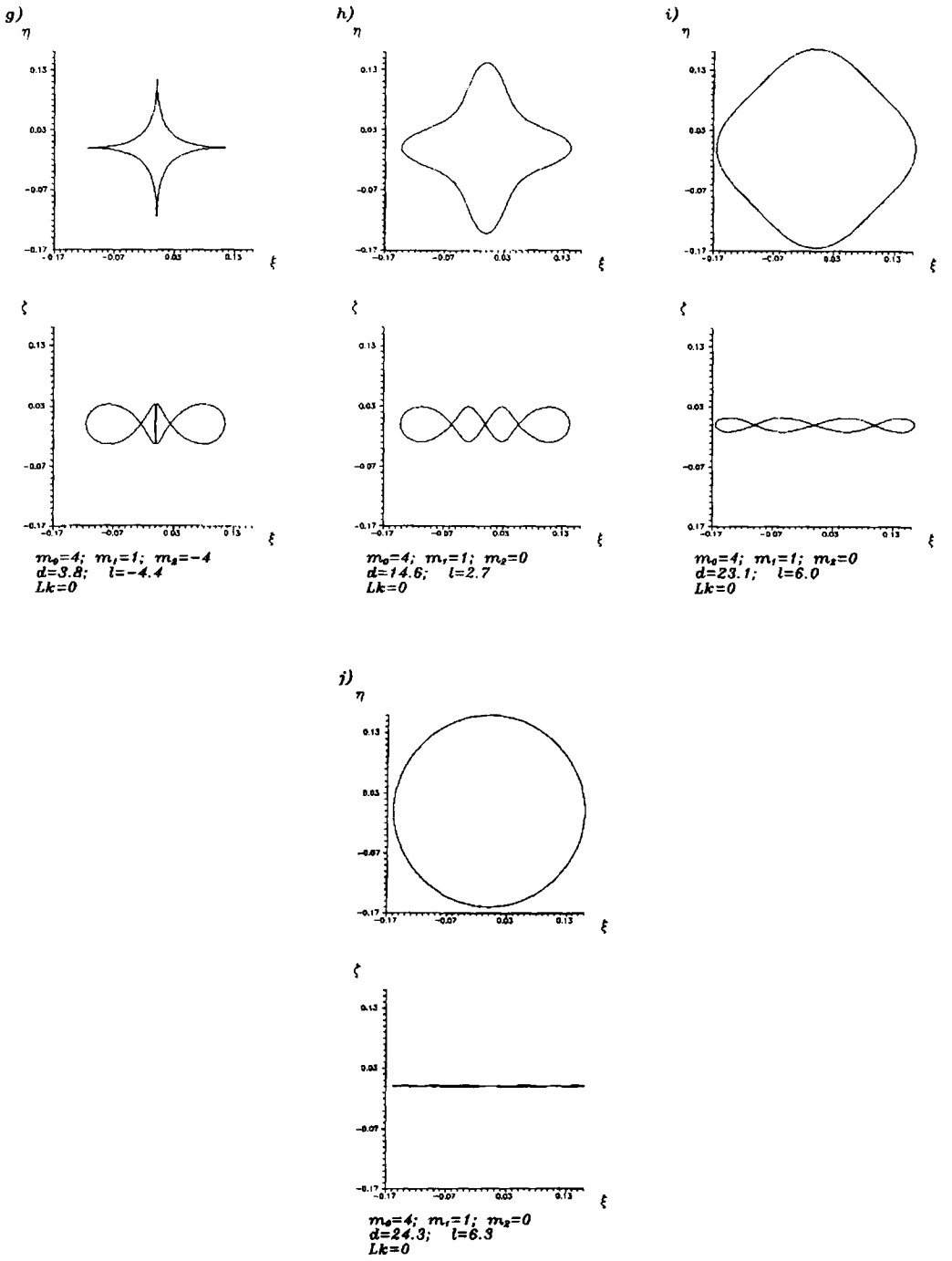

Figure 17. The projections of the central axis for various values of the parameter d for $m_0 = 4$.

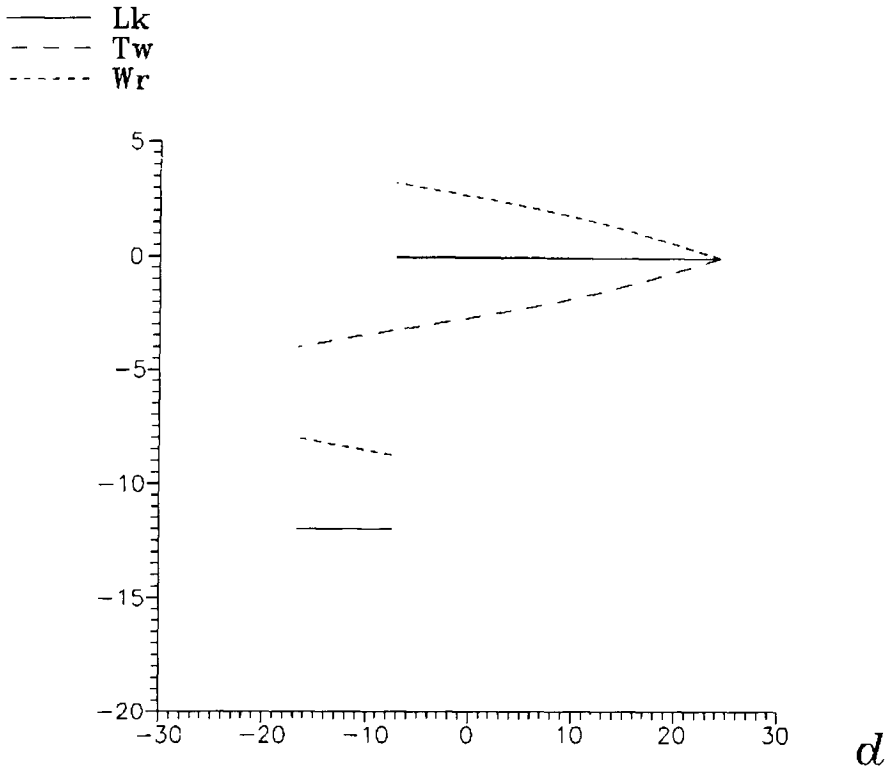

Figure 18. The linking, twisting and writhing numbers as functions of the parameter d for $m_0 = 4$.

to the lower branch of $\Phi(d)$ occurs (B4). Note that in both cases the number m_1 changes for $m_1 - m_0 \operatorname{sign} m_1$.

For $m_0 = 2$ the intersecting configuration coincides with that for which the function $\Phi(d)$ with fixed m_2 has the jump discontinuity ($l = -d = 0$). In order to make the curve $\Phi(d)$ continuous, the number m_2 must be changed by the value of $m_0 = 2$ (41) for the shape A4. Otherwise, the lower branch with unchanged $m_2 = 0$ is to be followed. The transformation proceeds further in the reverse order and eventually another plane ring is obtained with the following parameters:

$$l = 2\pi, \qquad d = 2\pi\sqrt{3}, \qquad h = 4\pi^2, \qquad p = 8\pi^2\sqrt{3} \qquad (m_0 = 2,\ m_1 = 1).$$

Both A6 and $B6$ are examples of the plane ring, but with different twists.

Small pictures in Figure 6 are zoomed in Figure 12 (A-sequence) and in Figure 13 (B-sequence) to show a transformation of the molecule in space more clearly. It is easy to see that the B-sequence is a mirror reflection of the A-sequence. Values of the parameter d are indicated under pictures.

All these transformations can readily be demonstrated by using the model made of a rubber hose. Since it is not easy to change the natural twist of such a model, the angle φ continuity condition should be abandoned, or more simply, two ends of the hose are to be joined together and slowly rotated around its central axis. The change of the angle of their mutual turn then simulates change of the natural twist value.

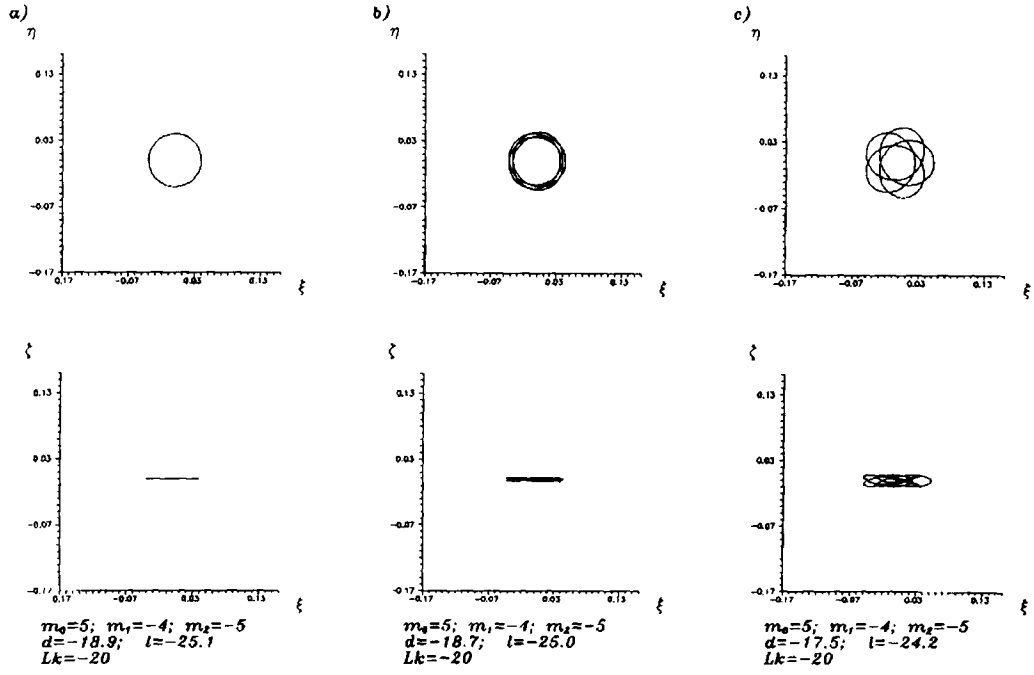

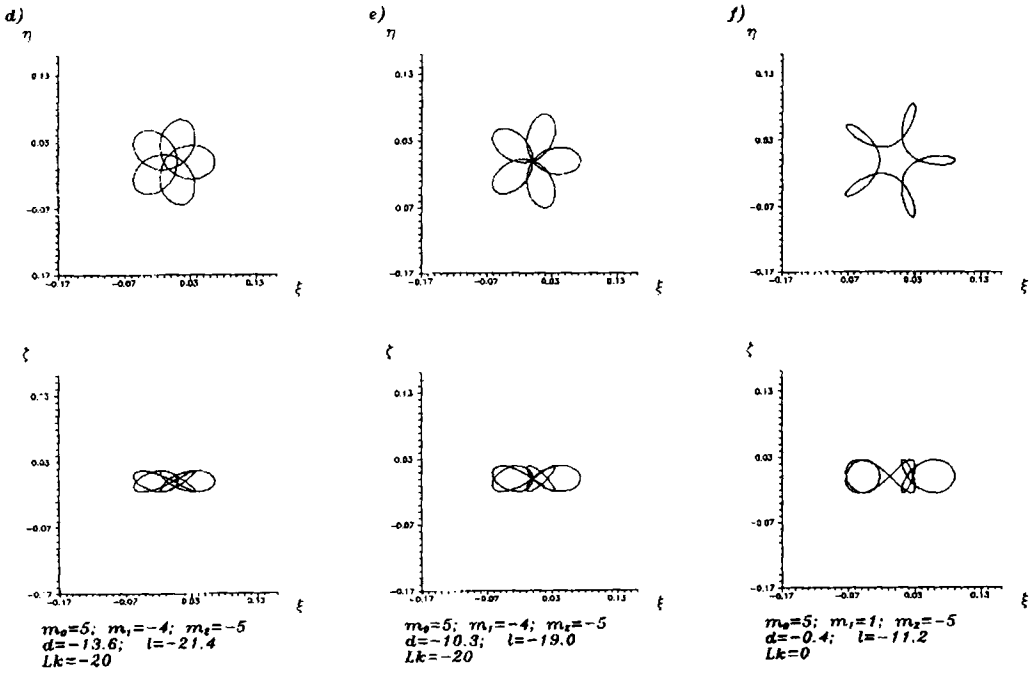

Figure 19. (cont.)

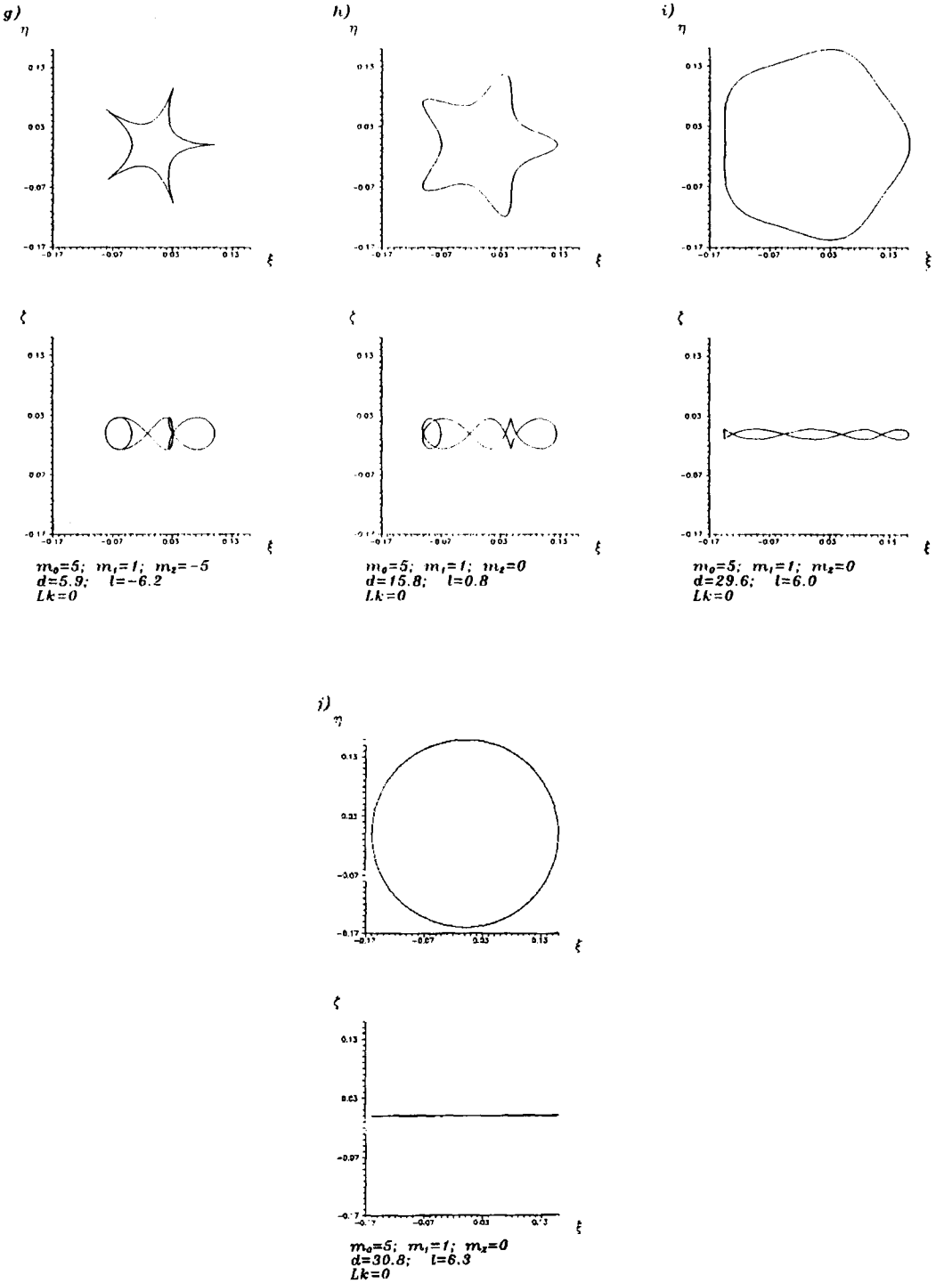

Figure 19. The projections of the central axis for various values of the parameter d for $m_0 = 5,\ m_1 = -4 \to 1$.

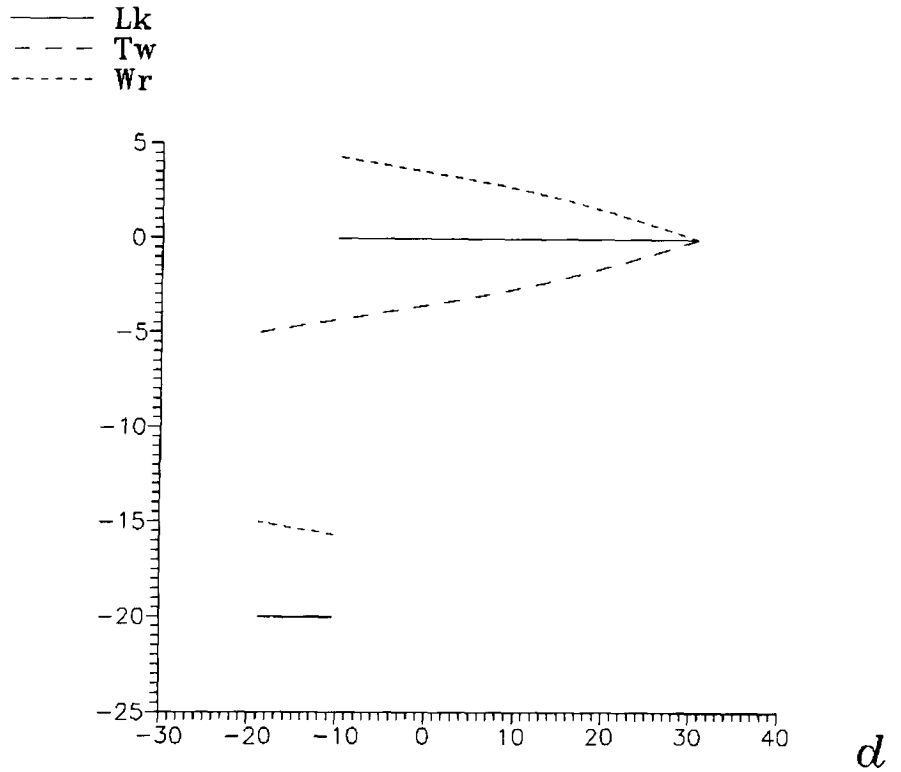

Figure 20. The linking, twisting and writhing numbers as functions of the parameter d for $m_0 = 5$, $m_1 = -4 \rightarrow 1$.

$m_0 = 3$. The situation in this case is rather similar to the previous one. Two branches of the curve $\Phi(d)$ are shown in Figure 14. Change of the central axis form may be observed in Figure 15 (a) to (j). Two projections of it are presented for different values of d. The values of m_2 and Lk under pictures are given for the lower branch of the curve $\Phi(d)$ while the values of other parameters and the projections are the same for the both curves. Only the case for $m_1 = -2 \rightarrow 1$ is shown; the second possible case $m_1 = -1 \rightarrow 2$ is just a mirror reflection.

Unlike the previous case $m_0 = 2$, here the jump discontinuity of $\Phi(d)$ and self-intersection occur at different values of d.

Figure 15 (e) corresponds to the conformation with triple self-intersection. The writhing and the linking change by 3+3=6 (Figure 16). The conformation is essentially spatial, but the computation shows that all its three loops may be considered planar and the writhing number may be easily evaluated by taking into account only the vicinity of the origin. The approach suggested in [8] for plane loops is readily extended to symmetrical shapes with multiple intersections at the origin.

The projection with three cusp points is shown in Figure 15(g). It corresponds to the change of m_2 in order to prevent the jump of $\Phi(d)$.

The sequence (a)–(j) starts and finishes with plane rings. The circle (a) is traced twice while the circle (j) is simple. The circles have different diameters, because the total length of the rod is fixed.

$m_0 = 4$. This case is presented in Figure 17 (a) – (j). The multiple self-intersection occurs for $l = -4\pi$ (see (42)). The projection of the central axis on the plane $\xi\eta$ has 8 crossing points

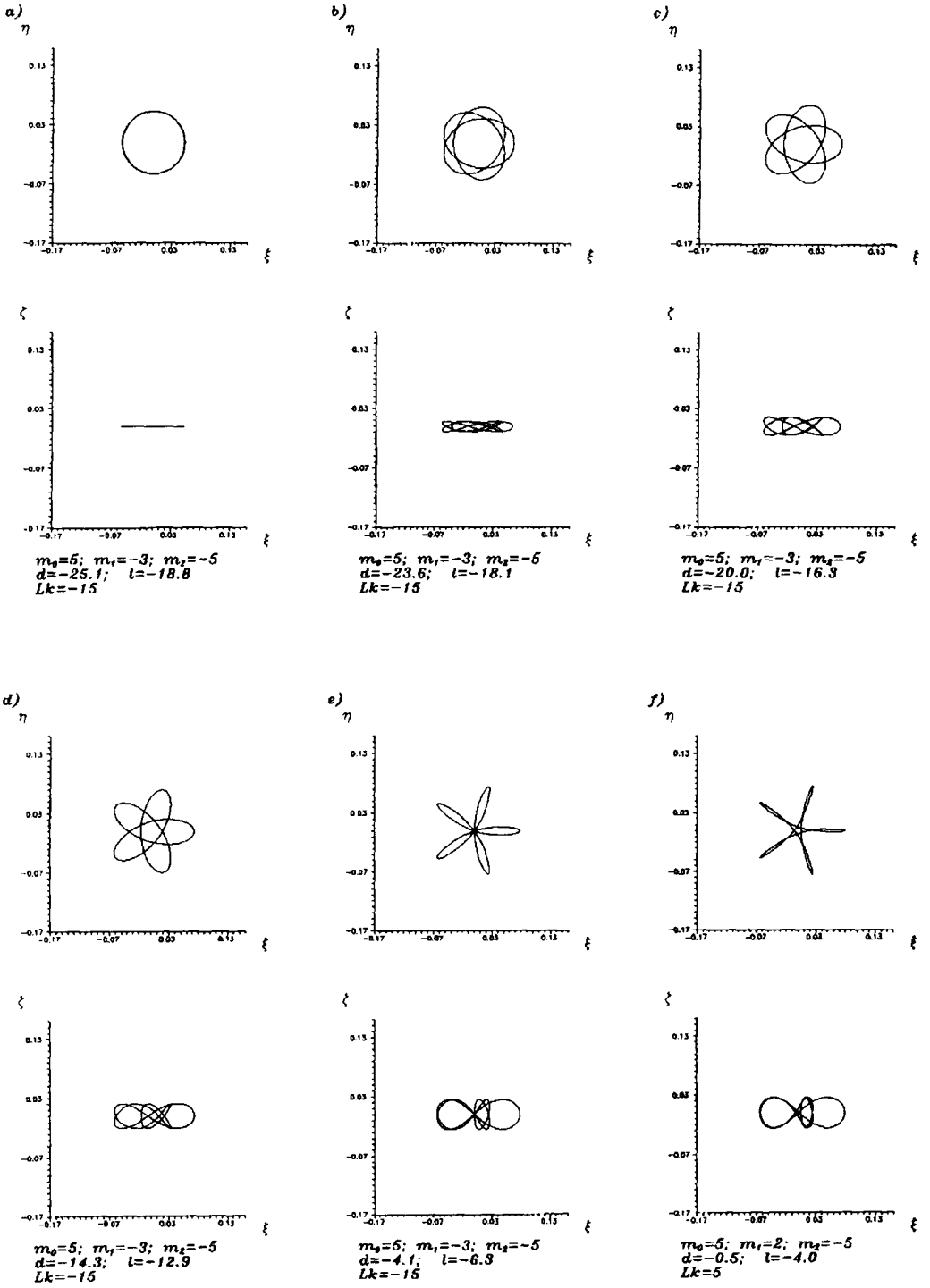

Figure 21. (cont.)

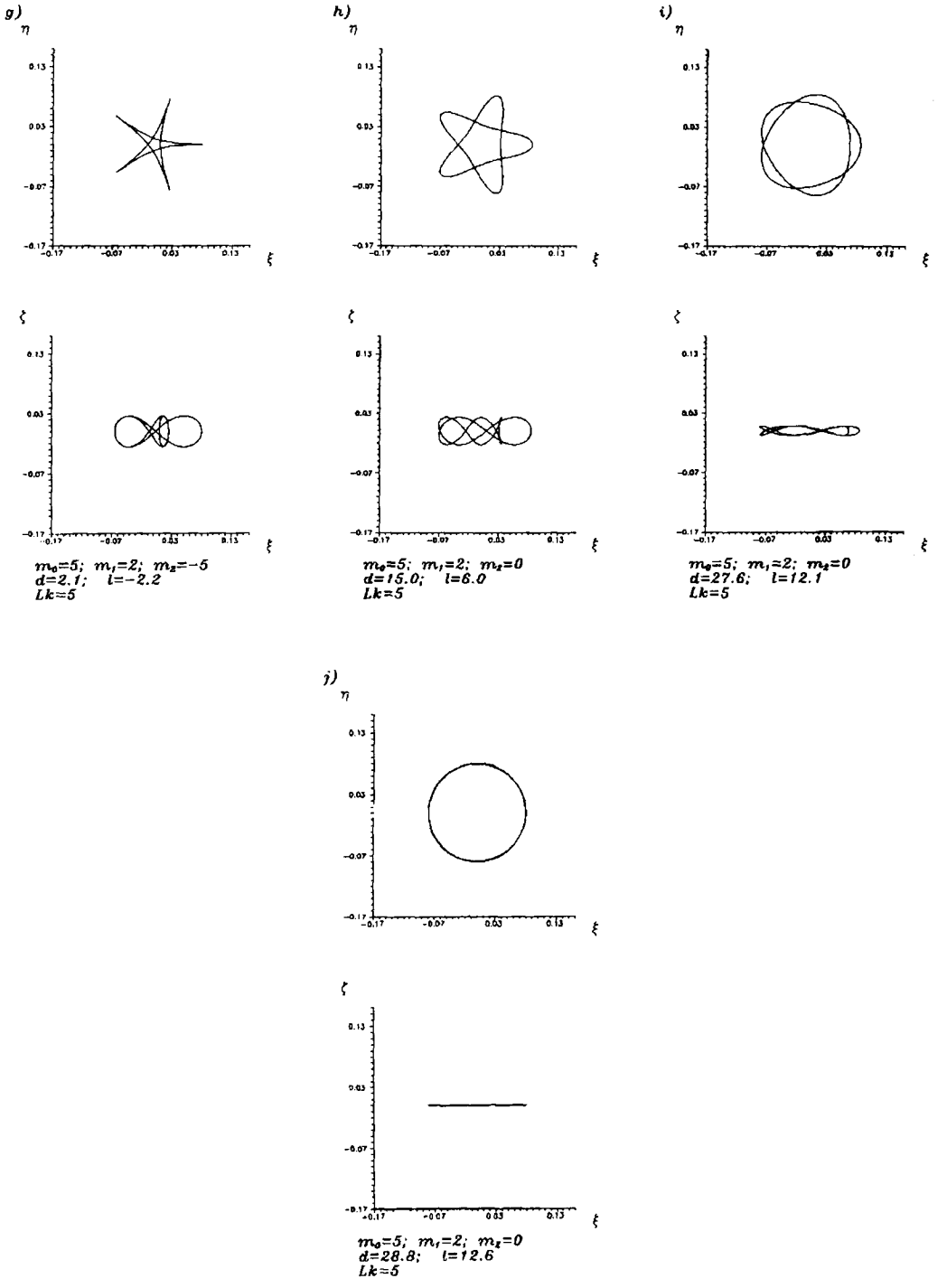

Figure 21. The projections of the central axis for various values of the parameter d for $m_0 = 5$, $m_1 = -3 \rightarrow 2$.

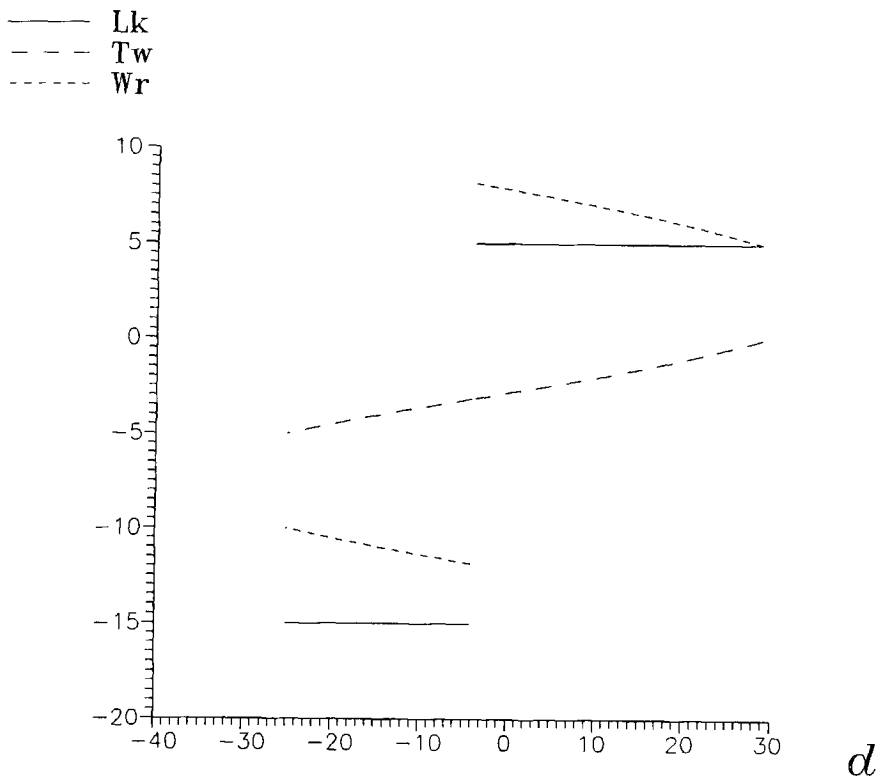

Figure 22. The linking, twisting and writhing numbers as functions of the parameter d for $m_0 = 5$, $m_1 = -3 \rightarrow 2$.

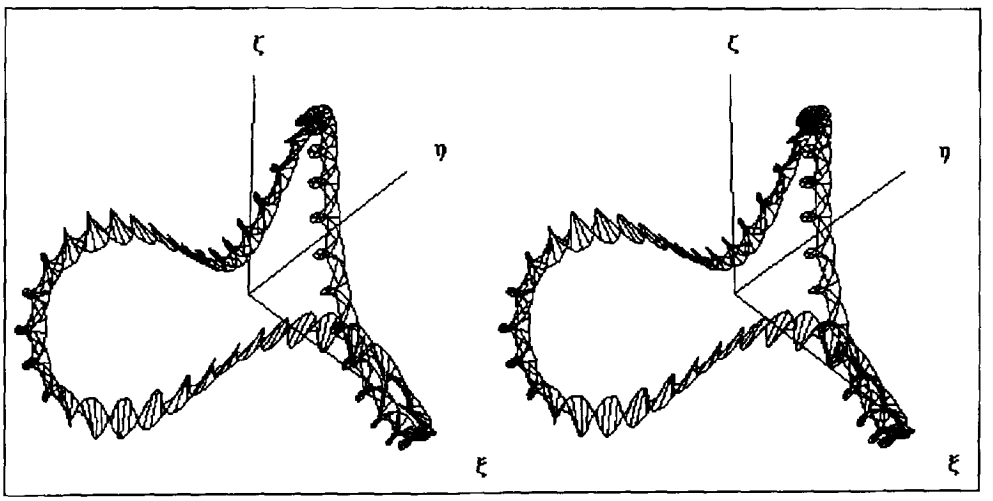

Figure 23. Stereo view of a closed molecule for $d = 8.6665$, $l = 2.1132$, $h = 221.68$, $p = 310.16$, $m_0 = 3$, $m_1 = 1$, $m_2 = 25$. The linking number $Lk = 25$, writhing $Wr = 1.08$, and twist $Tw = 23.92$.

before the self-intersection (d) and 4 crossing points after it (f). As m_1 changes its sign, the direction of counting of the polar angle is opposite for (d) and (f) pictures. Therefore the linking number must change by $8 + 4 = 12$ (Figure 18).

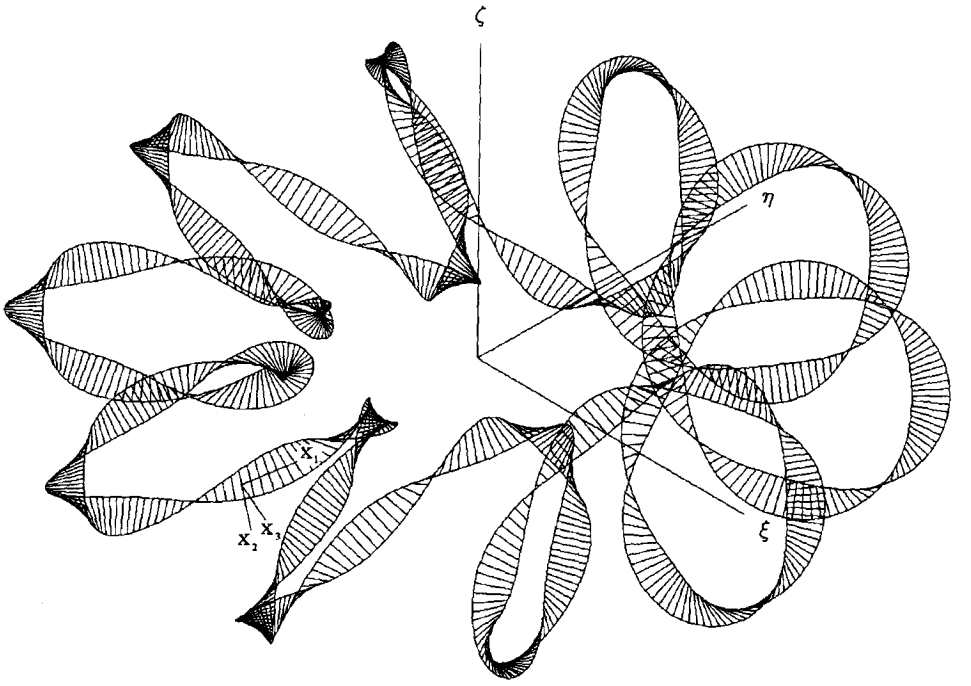

Figure 24. An example of the closed conformation for larger m_0; $d = -0.8, l = -29.8, h = 3537.6, p = 2583.0$, $m_0 = 10, m_1 = 1, m_2 = 20$, and $Lk = 30$.

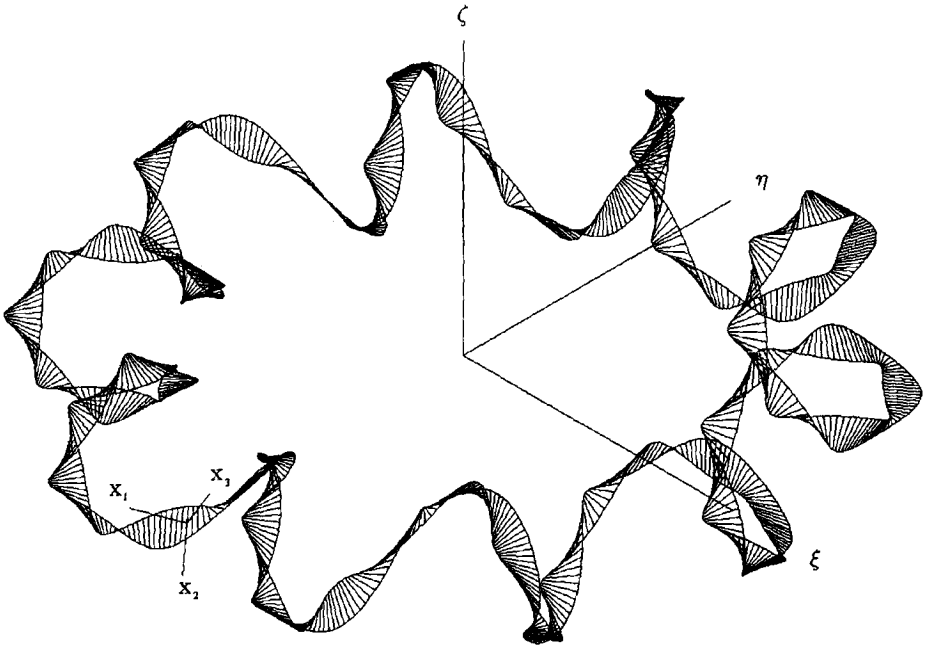

Figure 25. An example of the closed conformation for larger m_0; $d = 22.6, l = -7.1, h = 3207.8, p = 1756.1$, $m_0 = 10, m_1 = 1, m_2 = 30$, and $Lk = 30$.

As in the previous case, the sequence (a)–(j) starts and finishes with plane rings. The circle (a) is traced three times and the circle (j) once. The diameter of the ring (a) is one third of the diameter of (j).

$m_0 = 5$. There exist two essentially different cases. The corresponding sequences of the central axis projections are presented in Figures 19 ($m_1 = -4 \to 1$) and 21 ($m_1 = -3 \to 2$). The linking, twisting and writhing numbers as functions of d are plotted in Figures 20 and 22, respectively.

Both sequences (a)–(j) start and finish with plane rings, but the circle 19 (a) is traced four times while the circle 21 (a) three times. The ending circles 19 (j) and 21 (j) are traced once and twice, respectively.

The simplest families of configurations were considered. The behaviour of others with larger m_0 is more complicated.

The plots presented together with Equation (36) also allow for the possibility to see how the equilibrium shape of the closed molecule changes as the ratio of its twisting to the bending stiffness (the parameter b) slowly changes. This may be caused by the influence of the environment.

The proposed approach provides computation of spatial closed shapes starting with an arbitrary plane ring. As an example, Figure 23 shows a stereo view of a closed molecule for the following values of the parameters: $d = 8.7$, $l = 2.1$, $h = 221.7$, $p = 310.2$, $m_0 = 3$, $m_1 = 1$, $m_2 = 25$. Its linking number $Lk = 25$, writhing $Wr = 1.08$, and twist $Tw = 23.92$. (Note that much larger values of numbers m_i may be taken, in particular m_2 of order 10^2, which corresponds to real molecules, but then the picture would be less comprehensible.)

In order to give insight into the shapes of the molecule for larger m_0, two more intricate conformations are shown in Figure 24 ($d = -0.8$, $l = -29.8$, $h = 3537.6$, $p = 2583.0$, $m_0 = 10$, $m_1 = 1$, $m_2 = 20$) and Figure 25 ($d = 22.6$, $l = -7.1$, $h = 3207.8$, $p = 1756.1$, $m_0 = 10$, $m_1 = 1$, $m_2 = 30$). For both shapes, $Lk = 30$.

4. Concluding Remarks

An infinite number of families of essentially non-planar closed shapes were found for a closed DNA molecule modelled at large as a thin elasic rod. Necessary conditions on the parameters were obtained that allow one to find bifurcation points of non-planar equilibrium shapes from the plane ring. The method proposed provides effective means to compute a molecule shape in space for an arbitrary set of parameters and to analyze transformations as the parameters change. It is shown that the equation for the twist is decoupled from the equations determining the shape of the central axis of the molecule.

The approach may be extended to rod models with a non-symmetrical cross section ($B_{22} \neq B_{33}$) and initially curved. Although they are not integrable, the parameter continuation method may be applied starting with solutions of the integrable problem of the symmetrical and initially straight rod. Another problem to be solved is an investigation of stability properties of equilibrium conformations.

Investigation of DNA tertiary structure is important for understanding of DNA packing in bacteriophages and chromatin as well as of DNA functioning. However, the elastic rod model can be applied not only to DNA but to other long polymer molecules such as RNA and α-helix of protein as well. Also there exist many examples of stressed slender structures in different

fields of science and life and their intricate shapes can often be approximated by using rather simple mechanical assumptions.

5. Acknowledgements

I am grateful to Dr. E. I. Kugushev for stimulating discussions and valuable comments. This work was supported in part by Russian Foundation of Basic Research grant number 93-01-21914.

References

1. Crick, F. H. C., 'Linking numbers and nucleosomes', *Proc. Natl. Acad. Sci. USA*, **73** (8) (1976) 2639–2643.
2. Tsuru, H. and Wadati, M., 'Elastic model of highly supercoiled DNA', *Biopolymers*, **25** (1986) 2083–2096.
3. Bauer, W. R., Crick, F. H. C., White, J. H., 'Supercoiled DNA', *Scientific American*, **243** (1) July (1980) 100–113.
4. Benham, C. J., 'Elastic model of supercoiling', *Proc. Natl. Acad. Sci. USA*, **74** (1977) 2397–2401.
5. Le Bret, M., 'Catastrophic variation of twist and writhing of circular DNAs with constraint?', *Biopolymers*, **18** (1979) 1709–1725.
6. Benham, C. J., 'Geometry and mechanics of DNA superhelicity', *Biopolymers*, **22** (1983) 2477–2495.
7. Šelepová, P., Kypr, J., 'Computer simulation of DNA supercoiling in a simple elastomechanical approximation', *Biopolymers*, **24** (1985) 867–882.
8. Wadati, M. and Tsuru, H., 'Elastic model of looped DNA', *Physica* **21D** (1986) 213–216.
9. Tanaka, F. and Takahashi, H., 'Elastic theory of supercoiled DNA', *J. Chem. Phys.* **83** (11) (1985) 6017–6026.
10. Starostin, E. L., 'Three-dimensional conformations of looped DNA in an elastomechanical approximation'. In: Chien Wei-zang (ed.), *Proceedings of the 2nd International Conference on Nonlinear Mechanics*, Peking University Press, Beijing, 1993, pp. 188-190.
11. Love, A. E. H., *A Treatise on the Mathematical Theory of Elasticity* (4th edn), Cambridge University Press, 1927.
12. Tsuru, H., 'Nonlinear dynamics for thin elastic rod', *J. Phys. Soc. Japan*, **55** (7) (1986) 2177–2182.
13. Tsuru, H., 'Equilibrium shapes and vibrations of thin elastic rod', *J. Phys. Soc. Japan*, **56** (7) (1987) 2309–2324.
14. Domokos G., *A Group-Theoretic Approach to the Geometry of Elastic Rings*, Technical Note BN-1168, Institute for Physical Science and Technology, University of Maryland, 1994.
15. Cantor, C. R., Schimmel, P. R., *Biophysical Chemistry. Part III. The Behavior of Biological Macromolecules*, W. H. Freeman and Company, San Francisco, 1980.
16. Fuller, F. B., 'The writhing number of a space curve' *Proc. Natl. Acad. Sci. USA*, **68** (4) (1971) 815–819.
17. Barkley, M. D., Zimm, B. H., *J. Chem. Phys.* **70** (1979) 2992–3007.
18. Hogan, M., LeGrange, J. and Austin, B., 'Dependence of DNA helix flexibility on base composition', *Nature*, **304** (25) (1983) 752–754.
19. Landau, L. D. and Lifshitz, E. M., *Theory of Elasticity* (2nd edn), Pergamon, New York, Oxford, 1970.
20. Ilyukhin, A. A., *Spatial Problems of the Nonlinear Theory of Elastic Rods*, Naukova Dumka, Kiev, 1979 [in Russian].
21. Abramowitz, M. and Stegun, I. A., *Handbook of Mathematical Functions*, Dover, New York, 1972.